ISSN 2410-3454

Volume 11, Issue 32 — July — December — 2024

Journal of Engineering Applications

15th ANNIVERSARY ECORFAN Special Edition

Journal of Engineering Applications, Volume 11, Issue 32, December 2024, is a journal published biannual by ECORFAN - Bolivia. 21 Santa Lucía, CP-5220. Libertadores - Sucre - Bolivia. WEB: www.ecorfan.org, revista@ecorfan.org. Editor in Chief: JALIRICASTELLON, María Carla Konradis. PhD. ISSN-2410-3454. Responsible for the last update of this issue of the ECORFAN Informatics Unit. ESCAMILLA-BOUCHÁN, Imelda. PhD, LUNA-SOTO, Vladimir. PhD. Updated as of December 30, 2024.

Journal of Engineering Applications

Definition of Journal

Scientific Objectives

Support the international scientific community in its written production Science, Technology and Innovation in the Field of Engineering and Technology, in Subdisciplines of civil engineering, systems engineering, telecommunications engineering, electronic engineering, energy engineering, hydraulic engineering, industrial engineering, mechanical engineering, engineering, geological metallurgical, mining engineering, naval engineering, nuclear engineering, petroleum and petrochemical engineering, chemical engineering.

ECORFAN-Mexico, S.C. is a Scientific and Technological Company in contribution to the Human Resource training focused on the continuity in the critical analysis of International Research and is attached to CONAHCYT-RENIECYT number 1702902, its commitment is to disseminate research and contributions of the International Scientific Community, academic institutions, agencies and entities of the public and private sectors and contribute to the linking of researchers who carry out scientific activities, technological developments and training of specialized human resources with governments, companies and social organizations.

Encourage the interlocution of the International Scientific Community with other Study Centers in Mexico and abroad and promote a wide incorporation of academics, specialists and researchers to the publication in Science Structures of Autonomous Universities - State Public Universities - Federal IES -Polytechnic Universities - Technological Universities - Federal Technological Institutes - Normal Schools - Decentralized Technological Institutes - Intercultural Universities - S & T Councils – CONAHCYT Research Centers.

Scope, Coverage and Audience

Journal of Engineering Applications is a Journal edited by ECORFAN-Mexico, S.C. in its Holding with repository in Bolivia, is a scientific publication arbitrated and indexed with semester periods. It supports a wide range of contents that are evaluated by academic peers by the Double-Blind method, around subjects related to the theory and practice of civil engineering, systems engineering, telecommunications engineering, electronic engineering, energy engineering, hydraulic engineering, industrial engineering, mechanical engineering, engineering, geological metallurgical, mining engineering, naval engineering, nuclear engineering, petroleum and petrochemical engineering, chemical engineering with diverse approaches and perspectives, that contribute to the diffusion of the development of Science Technology and Innovation that allow the arguments related to the decision making and influence in the formulation of international policies in the Field of Engineering and Technology. The editorial horizon of ECORFAN-Mexico® extends beyond the academy and integrates other segments of research and analysis outside the scope, as long as they meet the requirements of rigorous argumentative and scientific, as well as addressing issues of general and current interest of the International Scientific Society.

Editorial Board

Arbitration Committee

Assignment of Rights

The sending of an Article to Journal of Engineering Applications emanates the commitment of the author not to submit it simultaneously to the consideration of other series publications for it must complement the Originality Format for its Article.

The authors sign the Authorization Format for their Article to be disseminated by means that ECORFAN-Mexico, S.C. In its Holding Bolivia considers pertinent for disclosure and diffusion of its Article its Rights of Work.

Declaration of Authorship

Indicate the Name of Author and Coauthors at most in the participation of the Article and indicate in extensive the Institutional Affiliation indicating the Department.

Identify the Name of Author and Coauthors at most with the CVU Scholarship Number-PNPC or SNI CONAHCYT- Indicating the Researcher Level and their Google Scholar Profile to verify their Citation Level and H index.

Identify the Name of Author and Coauthors at most in the Science and Technology Profiles widely accepted by the International Scientific Community ORC ID - Researcher ID Thomson - arXiv Author ID - PubMed Author ID - Open ID respectively.

Indicate the contact for correspondence to the Author (Mail and Telephone) and indicate the Researcher who contributes as the first Author of the Article.

Plagiarism Detection

All Articles will be tested by plagiarism software PLAGSCAN if a plagiarism level is detected Positive will not be sent to arbitration and will be rescinded of the reception of the Article notifying the Authors responsible, claiming that academic plagiarism is criminalized in the Penal Code.

Arbitration Process

All Articles will be evaluated by academic peers by the Double Blind method, the Arbitration Approval is a requirement for the Editorial Board to make a final decision that will be final in all cases. MARVID® is a derivative brand of ECORFAN® specialized in providing the expert evaluators all of them with Doctorate degree and distinction of International Researchers in the respective Councils of Science and Technology the counterpart of CONAHCYT for the chapters of America-Europe-Asia- Africa and Oceania.

The identification of the authorship should only appear on a first removable page, in order to ensure that the Arbitration process is anonymous and covers the following stages: Identification of the Journal with its author occupation rate - Identification of Authors and Coauthors - Detection of plagiarism PLAGSCAN - Review of Formats of Authorization and Originality-Allocation to the Editorial BoardAllocation of the pair of Expert Arbitrators-Notification of Arbitration -Declaration of observations to the Author-Verification of Article Modified for Editing-Publication.

Instructions for Scientific, Technological and Innovation Publication

Knowledge Area

The works must be unpublished and refer to topics of civil engineering, systems engineering, telecommunications engineering, electronic engineering, energy engineering, hydraulic engineering, industrial engineering, mechanical engineering, engineering, geological metallurgical, mining engineering, naval engineering, nuclear engineering, petroleum and petrochemical engineering, chemical engineering and other topics related to Engineering and Technology.

Presentation of the content

In the first article we present *Analysis of solution methods for high order ordinary differential equations used in electrical circuits* by Gutiérrez-Robles, José Alberto, Galván-Sánchez, Verónica Adriana, Bañuelos-Cabral, Eduardo Salvador and De La Cruz-García, Elba Lilia, with secondment at the University of Guadalajara, as a second article we present *Inverter technology and the role of the user behavior: Towards a more efficient use of energy* by Vidal-Santo, Adrián, Campos-Domínguez, Armando, Vázquez-Guzmán, Aldo G. and Castillo-Toscano, William A., with adscription in the Universidad Veracruzana, as third article we present *Methodological proposal for the topographic use of UAV compared to the use of traditional methods* by Rodríguez-González, José Miguel, Gómez-Arizmendi, Gabriela, Velázquez-García, Jennyfer and Carranza-Reyes, Roberto, with adscription at the Tecnológico Nacional de México/TES Valle de Bravo, as the fourth article we present *Study of the relationship between uniaxial compressive strength and the point load index test in rocks from the bank in Seybaplaya Campeche Mexico*, by Naal-Pech, José Wilber, Palemón-Arcos, Leonardo, El-Hamzaoui, Youness and Gutiérrez-Can, Yuriko, with adscription in the Universidad Autónoma del Carmen.

Content

Journal of Engineering Applications December 2024 Vol.11 No.32 1-19
Article

Analysis of solution methods for high order ordinary differential equations used in electrical circuits

Análisis de métodos de solución de ecuaciones diferenciales ordinarias de alto orden con aplicación en circuitos eléctricos

Gutiérrez-Robles, José Alberto [a], Galván-Sánchez, Verónica Adriana*[b], Bañuelos-Cabral, Eduardo Salvador[c] and De La Cruz-García, Elba Lilia[d]

[a] ROR University of Guadalajara • 0000-0002-0276-0244 • 30264
[b] ROR University of Guadalajara • 0000-0002-5462-2361 • 293960
[c] ROR University of Guadalajara • 0000-0002-6004-5898 • 241756
[d] ROR University of Guadalajara • 0009-0005-3018-1900

CONAHCYT classification:

Area: Physics-Mathematics and Earth Sciences
Field: Mathematics
Discipline: Numerical analysis
Subdiscipline: Ordinary differential equations

https://doi.org/10.35429/JEA.2024.32.11.1.19

History of the article:
Received: September 01, 2024
Accepted: December 26, 2024

Check for updates

* ✉ [veronica.galvan@academicos.udg.mx]

Abstract

This article presents a detailed methodology for applying the most common methods in solving high-order ordinary differential equations in the simulation of electrical circuits. The methods analyzed include the Laplace transform, the direct method in the time domain, the z-transform, the finite difference method, and methods based on difference equations. A detailed development of each of these methods is provided, along with practical examples that demonstrate their application in specific electrical circuits. The examples include: a circuit modeled with a second-order ordinary differential equation, a circuit modeled with a third-order ordinary differential equation, and an electrical network whose modeling results in an eighth-order ordinary differential equation. The article compares the results obtained with each method, using the Laplace transform solution as a reference. A deep analysis of the deviations between the methods is conducted, considering different time steps and parameters, allowing conclusions to be drawn about the effectiveness and accuracy of each approach.

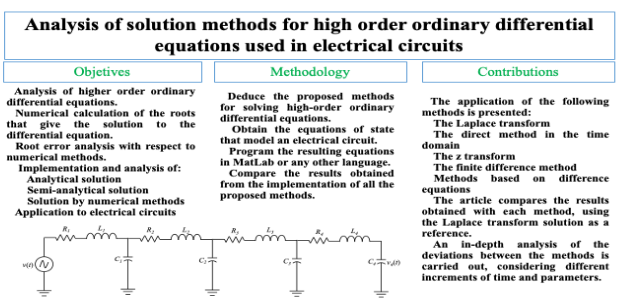

Differential equations, Laplace transform, Z-transform, Newton differences

Resumen

Este artículo presenta una metodología detallada para la aplicación de los métodos más comunes en la resolución de ecuaciones diferenciales ordinarias de alto orden en la simulación de circuitos eléctricos. Los métodos analizados incluyen la transformada de Laplace, el método directo en el dominio del tiempo, la transformada z, el método de diferencias finitas y los métodos basados en ecuaciones en diferencias. Se provee un desarrollo detallado de cada uno de estos métodos, acompañado de ejemplos prácticos que demuestran su aplicación en circuitos eléctricos específicos. Los ejemplos incluyen: un circuito modelado con una ecuación diferencial ordinaria de segundo orden, un circuito modelado con una ecuación diferencial ordinaria de tercer orden, una red eléctrica cuyo modelado resulta en una ecuación diferencial ordinaria de octavo orden. El artículo compara los resultados obtenidos con cada método, utilizando la solución de la transformada de Laplace como referencia. Se realiza un análisis profundo de las desviaciones entre los métodos, considerando diferentes incrementos de tiempo y parámetros, lo que permite llegar a conclusiones sobre la eficacia y precisión de cada enfoque.

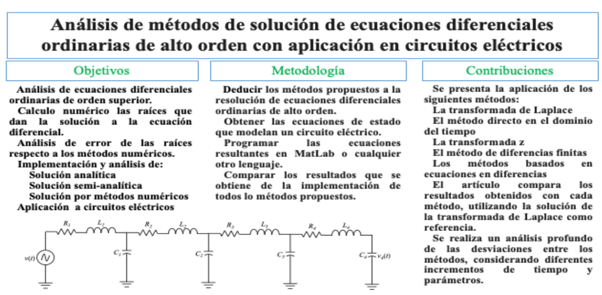

Ecuaciones diferenciales, Transformada de Laplace, transformada z, Diferencias de Newton

Citation: Gutiérrez-Robles, José Alberto, Galván-Sánchez, Verónica Adriana, Bañuelos-Cabral, Eduardo Salvador and De La Cruz-García, Elba Lilia. Analysis of solution methods for high order ordinary differential equations used in electrical circuits. Journal of Engineering Applications. 2024. 11-32: 1-19.

Journal of Engineering Applications December 2024 Vol.11 No.32 1-19
Article

Introduction

Most of the physical phenomena that can be modeled with physical-mathematical formulations evolve in space and/or in time. Although there is a wide range of phenomena that only evolve in space or in time. In a natural way, some systems have a dynamic that stores or transfers energy in some of all its forms; mechanical, kinetic, potential, gravitational, acoustic, electrical, thermal, chemical, magnetic, nuclear, radiant, wind, solar, hydraulic or light. The physical-mathematical relationships of these systems are commonly modeled using differential equations; either partial if it depends on more than one independent spatial or space-temporal variable (Xiang et. al.) and/or ordinary if it only depends on a single independent variable, whether spatial or temporal. On the other hand, for the case of systems that depend on a single variable; the number of elements that store or transfer energy defines the order of the equation or the size of the systems of equations that model the physical phenomenon (Salas et. al.).

This work focuses on the modeling of concentrated electrical systems (Lathi, B. P.), that is, that only evolve in time; thus, the resulting model will always be a high order ordinary differential equation (HOODE).

The solution methods that have been developed were initially applied to simple or low-order equations; thus, intuitively the first of them was developed by Leonard Euler. It is worth mentioning that Isaac Newton gave mathematical formality to integro-differential calculus, which is why the first formal analytical formulation occurred with the formation of group theory for differential equations. Obviously, Pierre-Simón Laplace, a century later, established the entire theory for the solution of this type of equations using what is now known as the Laplace transform.

Years later, the z-transform theory was developed, which is based on the series by Pierre Alphonse Laurent. From this theory a method called difference equations was developed that takes advantage of the discrete plane scheme obtained from the application of the z-transform.

Solution methods for high-order ordinary differential equations

Normally an ordinary differential equation is solved analytically; the main reason is that this result is associated with a more precise solution (Saadeh, R. et. al.) and (Golmankhaneh, A. K., & Bongiorno, D.). However, in the case of high-order ordinary differential equations (HOODE), the analytical solution involves calculating the roots of a polynomial of the same order as that of the differential equation, and this has to be done numerically, with no option. This calculation is quite sensitive. In fact, it is not predictable to know if the final result will have more error due to the calculation of the roots or to other types of implementations (Marciniak et. al.). For this reason, this section deals with the analytical solution, semi-analytical methods and numerical methods for the solution of a HOODE.

Analytical methods

There are two traditional ways of solving a high-order ordinary differential equation, such as the Laplace transform, (Hsu, H. P.) and (Wilcox, D. J.), and its direct solution in the time domain by applying some method such as the indeterminate coefficients (Burden, L. R. & Faires, J. D.) and (Hoffman, J. D.). In this section, both methods are briefly described as well as the semi-analytical method of the z transform (Noda, T. & Ramirez, A.) and some numerical methods such as that of equations in differences or finite differences (Williams, P. W.), (Kinkaid D. R. & Hayes L. J.), (Smith G. D.) and (Strikwerda J.).

Laplace transform

Consider the HOODE with constant coefficients of the form

$$\sum_{k=0}^{N} a_k w^{(k)} = f(t) \quad (1)$$

with $w^m(0) = w_0^m \quad 0 \le m \le M - 1$.

The Laplace transform of (1) has the following structure:

$$\sum_{k=0}^{N} \left(a_k s^k\right) W(s) - \sum_{k-0}^{N} \left(\sum_{j}^{k-1} s^{k-j-1} a_k w^{(j)}(0) \right) = F(s) \quad (2)$$

ISSN: 2410-3454.
RENIECYT-CONAHCYT: 1702902

Gutiérrez-Robles, José Alberto, Galván-Sánchez, Verónica Adriana, Bañuelos-Cabral, Eduardo Salvador and De La Cruz-García, Elba Lilia. Analysis of solution methods for high order ordinary differential equations used in electrical circuits. Journal of Engineering Applications. 2024. 11-32: 1-19
https://doi.org/10.35429/JEA.2024.32.11.1.19

Taking into account the initial conditions and clearing $W(s)$ from (2) we arrive at,

$$W(s)=\frac{F(s)+\sum_{k-0}^{N}\left(\sum_{j}^{k-1}s^{k-j-1}a_k w^{(j)}(0)\right)}{\sum_{k=0}^{N}\left(a_k s^k\right)} \quad (3)$$

The solution is obtained by algebraically expanding (3) to have simple elements to which the inverse Laplace transform is applied and arrive at a solution of the form,

$$w(t)=L^{-1}\{W(s)\} \quad (4)$$

Time domain solution

The direct solution of (1) is divided into two parts: in the first part the equation is equal to zero and it is proposed that the solution be of the type (homogeneous solution),

$$w(t)=w_t=e^{rt} \quad (5)$$

Thus, we have that the successive derivatives are of the form,

$$w_t^{(k)}=r^k e^{rt} \quad (6)$$

For $0\le k\le N$, by substituting (1) the characteristic polynomial or auxiliary equation is obtained,

$$\sum_{k=0}^{N}a_k r^k e^{rt}=e^{rt}\sum_{k=0}^{N}a_k r^k=0 \quad (7)$$

Since $e^{rt}\neq 0$, then the sum is necessarily equal to zero; Therefore, by means of the fundamental theorem of algebra, there are n solutions (roots) to the HOODE grouped in the following way,

$$w_t=\sum_{k=0}^{N}c_k r^{r_k t}=0 \quad (8)$$

The second part of the solution has to do with the $f(t)$ of the equation (particular solution). Here a function of the same type is proposed as $f(t)$ and the coefficients that adjust it are found. The sum of both solutions, homogeneous and particular, make up the total solution of the differential equation.

Semi-Analytical methods

It can be said that the z-transform method is semi-analytical since it starts from an analytical methodology until it reaches a numerical representation. The transformation technique is an important tool in the analysis of signals and linear systems that are invariant in time (ITLS). The z transform provides a means of characterizing ITLS and their response to various signals by the positions of their poles and zeros. The z-transform of a discrete signal in time is defined as the power series as,

$$X(z)=\sum_{n=-\infty}^{\infty}x(n)z^{-n} \quad (9)$$

where z is a complex variable denoted by $z=Ae^{j\omega}$. The previous relationship is called direct z-transform, since it transforms the signal $x(n)$ in the complex plane $X(z)$,

$$X(z)=Z\{x(n)\} \quad (10)$$

Note that the z-transform is an infinite power series, therefore, it only exists for those values of z for which the series converges.

To carry out the inverse transformation of an equation in the z-plane, the partial fraction technique will be used, so we can express the function $X(z)$, as a linear combination,

$$X(z)=\sum_{k=1}^{N}a_k X_k(z), \quad (11)$$

where $X_k(z)$ are expressions whose inverse transformations are $x_k(n)$. If such decomposition is possible, then $x(n)$ it is the inverse z-transform of $X(z)$, by linear combination of,

$$x(n)=\sum_{k=1}^{N}a_k x_k(n) \quad (12)$$

This method is particularly useful if $X(z)$ it is a rational function, that is

$$X(z)=\frac{N(z)}{D(z)} \quad (13)$$

ISSN: 2410-3454.
RENIECYT-CONAHCYT: 1702902

Gutiérrez-Robles, José Alberto, Galván-Sánchez, Verónica Adriana, Bañuelos-Cabral, Eduardo Salvador and De La Cruz-García, Elba Lilia. Analysis of solution methods for high order ordinary differential equations used in electrical circuits. Journal of Engineering Applications. 2024. 11-32: 1-19
https://doi.org/10.35429/JEA.2024.32.11.1.19

Where it is necessary that the denominator be of the form $D(z)=1+a_1z^{-1}+L+a_Nz^{-N}$.

For simplification it is multiplied $D(z)$ by the one z^N where it $-N$ corresponds to the greatest negative power, this in order not to have negative powers in the denominator, so we have,

$$X(z)=\frac{\sum_{k=0}^{M}b_kz^{N-k-1}}{z^N+\sum_{k=1}^{N}a_kz^{N-k}} \quad (14)$$

For this purpose, we first decompose $D(z)$ into factors containing the poles p_k of $X(z)$.

We have the cases of distinct poles, repeated poles, and conjugated complex poles; in this way, for the case where the poles are different, we have

$$X(z)=\sum_{k=1}^{N}\frac{A_k}{1-p_kz^{-1}} \quad (15)$$

and the inverse z-transform of $X_k(z)$ is obtained by equivalence $Z^{-1}\{X_k(z)\}=(p_k)^n u(n)$, therefore

$$x(n)=u(n)\sum_{k=1}^{N}A_k(p_k)^n \quad (16)$$

For the case where we have multiplicity poles, the inverse transform is of the form,

$$Z^{-1}\left\{\frac{pz^{-1}}{\left(1-pz^{-1}\right)^k}\right\}=n^{k-1}p^nu(n) \quad (17)$$

In the case where we have some complex conjugated poles then complex exponentials are produced; However, if the signal $x(n)$ is real, it is possible to reduce said terms in real components; if we suppose that for some j between 1 and N they are had p_j and p_j^* in such a way that,

$$x_j(n)=\left[A_j(p_j)^n+A_j^*(p_j^*)^n\right]u(n) \quad (18)$$

and its combination in real components is,

$$x_j(n)=2|A_j|(r_j)^n\cos(nb_j+a_j)u(n) \quad (19)$$

where $A_j=|A_j|e^{ia_j}$ and $p_j=r_je^{ib_j}$. Thus, each z-domain conjugated complex pair produces a causal sinusoidal signal with an exponential envelope.

For the case where we have a differential equation of the type,

$$\sum_{k=1}^{N}a_k\frac{d^kw}{dt^k}=f(t) \quad (20)$$

the Laplace transform is applied first and the transition $W(s)\rightarrow W(z)$ and $s\rightarrow z$ is made by means of the trapezoidal or tustin rule $Z(s)=\frac{2}{\Delta t}\frac{z-1}{z-1}$ so, we have,

$$\mathrm{W}(z)=\frac{\sum_{m=0}^{M}\mathrm{B}_m\mathrm{z}^{-m}}{\sum_{k=0}^{N}\mathrm{A}_k\mathrm{z}^{-k}}=\frac{\beta_0+\mathrm{z}^{-1}\beta_1+\cdots+\mathrm{z}^{-M}\beta_M}{\alpha_0+\mathrm{z}^{-1}\alpha_1+\cdots+\mathrm{z}^{-N}\alpha_N} \quad (21)$$

and thus, the inverse z-transform is found as $w(n)=Z^{-1}\{W(z)\}$

Numerical methods

The numerical implementation of a high-order ordinary differential equation is done through finite differences; the first derivative is approximated with,

$$w_n'=\frac{w_{n+1}-w_n}{h} \quad (22)$$

The above for a given value of *h*. From (23) a recursive form for a derivative of order *N* can be obtained as follows,

$$w^{(N)}=\sum_{k=0}^{N}\binom{N}{k}\frac{(-1)^k}{h^N}w_{n+N-k} \quad (23)$$

A linear differential equation of order N has the form,

ISSN: 2410-3454.
RENIECYT-CONAHCYT: 1702902

Gutiérrez-Robles, José Alberto, Galván-Sánchez, Verónica Adriana, Bañuelos-Cabral, Eduardo Salvador and De La Cruz-García, Elba Lilia. Analysis of solution methods for high order ordinary differential equations used in electrical circuits. Journal of Engineering Applications. 2024. 11-32: 1-19
https://doi.org/10.35429/JEA.2024.32.11.1.19

$$\sum_{k=0}^{N} a_k w^{(k)}(t) = f(t) \qquad (24)$$

so, the difference scheme for this equation is,

$$\sum_{k=0}^{N} \sum_{j=0}^{k} \binom{k}{j} \frac{a_k (-1)^j}{h^k} w_{n+k-j} = f_n \qquad (25)$$

clearing for w_{n+N} then the following relation is obtained

$$w_{n+N} = \frac{h^N}{a_N}\left(f_n - \sum_{k=0}^{N-1} \sum_{j=0}^{k} \binom{k}{j} \frac{a_k (-1)^j}{h^k} w_{n+k-j} - \sum_{j=1}^{N} \binom{N}{j} \frac{a_N (-1)^j}{h^N} w_{n+N-j} \right) \qquad (26)$$

For a concurrence with an equation of order, initial conditions are necessary, which generates a unique solution to the differential equation (1).

Equations in differences

When constructing the mathematical model of some phenomenon, numerical and computational questions are interested, choosing a variable with discrete values. These data would be elements of a finite set, or failing that, a countable infinite. For this type of discrete deterministic models, the most appropriate mathematical tools to analyze them are the difference equations whose expression is of the type,

$$F\left(w_{n+N}, w_{n+N-1}, \ldots, w_{n+1}, w_n, n\right) = 0 \qquad (27)$$

where the order of this equation is the value of the difference between the largest with the smallest of the indices of *F*. A difference equation is said to be linear with constant coefficients if it can be written as,

$$\sum_{k=0}^{N} a_k w(n+k) = f(n) \qquad (28)$$

where $a_k \hat{I} R$. The objective is to find a function $w(n)$ that verifies that the equation for different values takes given values c_j, such that the solution is unique.

This is a fundamental system of solutions of the equation in differences, where the total solution is a linear combination of these, that is, if $\{w_1, w_2, \ldots, w_k\}$ are solutions, then the combination is solution too. So, we have,

$$w(n) = \sum_{j=1}^{k} c_j w_j(n) \qquad (29)$$

For the equation in difference with $f(n) = 0$, a solution of the type $w(n) = r^n$ is sought, so when substituting the solution in the equation we have,

$$\sum_{k=o}^{N} a_k r^{n+k} = r^N \sum_{k=o}^{N} a_k r^k = 0 \qquad (30)$$

which implies that,

$$\sum_{k=o}^{N} a_k r^k = 0 \qquad (31)$$

where r^k are the roots of the equation in difference. These roots can be simple, repeated or complex conjugated. So, the solution with $f(n) = 0$ is,

$$w_h(n) = r_1^n p_{m-1}(n) + \sum_{k=m+1}^{N-2} c_k r_k^n + r^n \left(b_1 cos(qn) + b_2 sen(qn)\right) \qquad (32)$$

with a single pair of complex conjugated roots $r_{1,2} = a \pm ib$ where $p = |r|$ and $\theta = \arctan(b/a)$. There is also $P_{m-1}(n) = c_1 + c_2 n + L + c_m n^{m-1}$ where the degree depends on the multiplicity of the roots. To find the complete solution it is necessary to estimate the particular solution which depends on the nature of the function $f(n)$ defined in the equation in difference.

Equation in differences from z

The equation in differences starting from the transfer function in *z* is,

ISSN: 2410-3454.
RENIECYT-CONAHCYT: 1702902

$$H(z)=\frac{W(z)}{F(z)} = \frac{k_N z^N + k_{N-1} z^{N-1} + L + k_1 z + k_0}{c_M z^M + c_{M-1} z^{M-1} + L + c_1 z + c_0} \quad (33)$$

where M and N are the degree of the numerator and denominator respectively, generally if the bilinear transformation given by the trapezoidal rule is used, these are the same. So, multiplying by z^{-N} you get to,

$$W(z)\left[c_N + c_{N-1}z^{-1} + L + c_1 z^{-N+1} + c_0 z^{-N}\right] = F(z)\left[k_N + k_{N-1}z^{-1} + L + k_1 z^{-N+1} + k_0 z^{-N}\right] \quad (34)$$

therefore, in differences we have,

$$c_N W_n + c_{N-1} W_{n-1} + L + c_1 W_{n-N+1} + c_0 W_{n-N} = k_N F_n + k_{N-1} F_{n-1} + L + k_1 F_{n-N+1} + k_0 F_{n-N} \quad (35)$$

Equation in differences from finite newton differences

A linear differential equation $\sum_{k=0}^{N} a_k w^{(k)}(t) = f(t)$ of order N expressed in finite differences has the form,

$$\sum_{k=0}^{N} \sum_{j=0}^{k} \binom{k}{j} \frac{a_k (-1)^j}{h^k} w_{n+k-j} = f_n \quad (36a)$$

so, if we expand all the terms and group them algebraically, we will have an equation of the type

$$a_N w_n + a_{N-1} w_{n-1} + L + a_1 w_{n-N+1} + a_0 w_{n-N} = f_n \quad (36b)$$

Application examples

The solution of a high-order ordinary differential equation depends mainly on the solution of its characteristic polynomial. Because there are only methods for calculating roots in an analytical way up to 5rd order, then a strictly analytical exact solution can only be obtained up to that order.

In this section some cases will be analyzed. The first one will be a 2nd order equation with exact roots, in this way the analytical solution will be exact, strictly speaking. The second will be a 3rd order equation with arbitrary solutions. The third example will be a fictitious circuit that is represented by an 8th order equation.

In the first case the initial conditions are defined to implement all the methods, but for the other cases the initial conditions are obtained for the conditions of the case.

First example

This example is constructed from the roots, that means, the exact solution of the representative polynomial is known a priori, for that reason it is possible to construct the analytical solution in exact form. The HOODE is,

$$a_2 \frac{d^2 v}{dt^2} + a_1 \frac{dv}{dt} + a_0 v = A\cos(\omega t) + B\sin(\omega t) + C$$

with

$a_2 = 1, a_1 = 6, a_0 = 8, A = 2, B = 3, C = 1, \omega = 2\pi f$, $f = 1/\pi$ and $T_{obs} = 8$ seconds. The initial conditions are $v(0) = 0$ and $v'(0) = 0$. The roots for this equation are $r_1 = -4$ and $r_2 = -2$.

Using the Laplace transforms

Applying the Laplace to the HOODE and taking into account the initial conditions, one obtain:

$$a_2\left(s^2V(s) - sv(0) - v'(0)\right) + a_1\left(sV(s) - v(0)\right) + a_0 V(s) = \frac{As}{s^2+\omega^2} + \frac{B\omega}{s^2+\omega^2} + \frac{C}{s}$$

So, the transfer function is,

$$H(s) = \frac{(A+C)s^2 + B\omega s + C\omega^2}{s^5 + 6s^4 + 12s^3 + 24s^2 + 32s}$$

Decomposing in partial fractions and solved we obtain

$$H(s) = \frac{0.175}{s+4} - \frac{0.125}{s+2} + \frac{0.125}{s} + \frac{-0.087-0.112i}{s-2i} + \frac{-0.087+0.112i}{s+2i}$$

Finally in time domain we have

$$v(t) = 0.175e^{-4t} - 0.125e^{-2t} + 0.125 + 2e^{-0t}\left(-0.087\cos(\omega t) + 0.112\sin(\omega t)\right)$$

Time domain solution

The HOODE is,

ISSN: 2410-3454.
RENIECYT-CONAHCYT: 1702902

Gutiérrez-Robles, José Alberto, Galván-Sánchez, Verónica Adriana, Bañuelos-Cabral, Eduardo Salvador and De La Cruz-García, Elba Lilia. Analysis of solution methods for high order ordinary differential equations used in electrical circuits. Journal of Engineering Applications. 2024. 11-32: 1-19
https://doi.org/10.35429/JEA.2024.32.11.1.19

Journal of Engineering Applications December 2024 Vol.11 No.32 1-19
Article

$$a_2 \frac{d^2v}{dt^2} + a_1 \frac{dv}{dt} + a_0 v = A\cos(\omega t) + B\sin(\omega t) + C$$

The proposed solution in time domain is as follows,
$$v_T(t) = v_h(t) + v_p(t) = c_1 e^{-4t} + c_2 e^{-2t} + b_1 cos(\omega t) + b_2 sen(\omega t) + b_3$$

Time domain particular solution

The particular proposed solution is as follows,

$$v_p(t) = b_1 \cos(\omega t) + b_2 \sin(\omega t) + b_3$$
$$v'_p(t) = -\omega b_1 \sin(\omega t) + \omega b_2 \cos(\omega t)$$
$$v''_p(t) = -\omega^2 b_1 \cos(\omega t) - \omega^2 b_2 \sin(\omega t)$$

Substituting in the ordinary differential equation (ODE), we obtain

$$\begin{bmatrix} b_1 \\ b_2 \\ b_3 \end{bmatrix} = \begin{bmatrix} -\omega^2 a_2 + a_0 & a_1\omega & 0 \\ -\omega^2 a_2 + a_0 & -\omega^2 a_2 + a_0 & 0 \\ 0 & 0 & a_0 \end{bmatrix}^{-1} \begin{bmatrix} A \\ B \\ C \end{bmatrix}$$

which solution yield to

$$v_p(t) = -0.175\cos(\omega t) + 0.225\sin(\omega t) + 0.125$$

Time domain homogenous solution

Using this solution, we have
$$v_T(t) = c_1 e^{-4t} + c_2 e^{-2t} - 0.175\cos(\omega t) + 0.225\sin(\omega t) + 0.125$$
$$v'_T(t) = -4c_1 e^{-4t} - 2c_2 e^{-2t} + \omega 0.175\cos(\omega t) + \omega 0.225\sin(\omega t)$$

So, we construct the system of algebraic equations using the initial conditions as

$$\begin{bmatrix} c_1 \\ c_2 \end{bmatrix} = \begin{bmatrix} 1 & 1 \\ -4 & -2 \end{bmatrix}^{-1} \begin{bmatrix} 0.175\cos(0) - 0.225\sin(0) - 0.125 \\ -\omega 0.175\cos(0) - \omega 0.225\sin(0) \end{bmatrix}$$

Finally, we obtain $c_1 = 0.175$ and $c_2 = -0.125$. So, the solution is:
$$v_T(t) = 0.175e^{-4t} - 0.125e^{-2t} - 0.175\cos(\omega t) + 0.225\sin(\omega t) + 0.125$$

Z-transform solution

The solution in z-plane is constructed from $H(s)$, so we have

$$H(s) = \frac{(A+C)s^2 + B\omega s + C\omega^2}{s^5 + 6s^4 + 12s^3 + 24s^2 + 32s}$$

Then, by using MatLab to construct Hz; first it is used the instruction "Hs=tf([Ns], [Ds])" which creates a continuous-time transfer function SYS as Hs=tf([(A+C) ω*B ω 2C], [1 6 12 24 32 0]).

Having Hs, we use c2d to compute a discrete time model Hz, with sample time h, and with the trapezoidal rule (tustin) that approximates the continuous time model.

Hz = c2d(Hs,h,'tustin')

$$H(z) = \frac{W(z)}{F(z)} = \frac{k_5 z^5 + k_4 z^4 + k_3 z^3 + k_2 z^2 + k_1 z + k_0}{c_5 z^5 + c_4 z^4 + c_3 z^3 + c_2 z^2 + c_1 z + c_0}$$

Finally, we use the function "residuez" to find the z-transform partial-fraction expansion of N(z)/D(z), so we obtain the residues, poles and direct term as

[r,p,Kp]=residuez(Hz.Numerator{1}, Hz.Denominator{1})

We construct the solution of the HOODE in z-domain as,
$$v(t) = \frac{r_1(p_1)^{ke} + r_2(p_2)^{ke} + r_3(p_3)^{ke} + r_4(p_4)^{ke} + r_5(p_5)^{ke}}{h}$$

with

$1 \le ke \le n-1$ and $n =$ number of samples. The first sample is corrected with the direct term as, $v(1) = v(1) + \frac{Kp}{h}$.

Equation in differences solution from z

The solution begins with the transfer function of the left side of the differential equation, so we have

$$H(s) = \frac{1}{s^2 + 6s + 8}$$

by using this, in z-domain we obtain

$$H(z) = \frac{W(z)}{F(z)} = \frac{[N_1 z^2 + N_2 z + N_3]}{[D_1 z^2 + D_2 z + D_3]} = \frac{z^{-2}}{z^{-2}}$$

Re-arranging we arrives to

$$V(z)[D_1 + D_2 z^{-1} + D_3 z^{-2}] = F(z)[N_1 + N_2 z^{-1} + N_3 z^{-2}]$$

So we have

ISSN: 2410-3454.
RENIECYT-CONAHCYT: 1702902

Gutiérrez-Robles, José Alberto, Galván-Sánchez, Verónica Adriana, Bañuelos-Cabral, Eduardo Salvador and De La Cruz-García, Elba Lilia. Analysis of solution methods for high order ordinary differential equations used in electrical circuits. Journal of Engineering Applications. 2024. 11-32: 1-19
https://doi.org/10.35429/JEA.2024.32.11.1.19

$$D_1V_n + D_2V_{(n-1)} + D_3V_{(n-2)} = N_1F_n + N_2F_{(n-1)} + N_3F_{(n-2)}$$

Particular solution

Solving for the particular proposed solution, we obtain

$$V_n = k_1\cos\left(M\Delta tn\right) + k_2\sin\left(M\Delta tn\right) + k_3$$

$$V_{(n-1)} = k_1\cos\left(M\Delta t\left(n-1\right)\right) + k_2\sin\left(M\Delta t\left(n-1\right)\right) + k_3$$

$$V_{(n-1)} = k_1\cos\left(M\Delta tn\right)\cos\left(M\Delta t\right) + k_1\sin\left(M\Delta tn\right)\sin\left(M\Delta t\right) + k_2\sin\left(M\Delta tn\right)\cos\left(M\Delta t\right) - k_2\cos\left(M\Delta tn\right)\sin\left(M\Delta t\right) + k_3$$

$$V_{(n-2)} = k_1\cos\left(M\Delta t\left(n-2\right)\right) + k_2\sin\left(M\Delta t\left(n-2\right)\right) + k_3$$

$$V_{(n-2)} = k_1\cos\left(M\Delta tn\right)\cos\left(2M\Delta t\right) + k_1\sin\left(M\Delta tn\right)\sin\left(2M\Delta t\right) + k_2\sin\left(M\Delta tn\right)\cos\left(2M\Delta t\right) - k_2\cos\left(M\Delta tn\right)\sin\left(2M\Delta t\right) + k_3$$

and

$$F_n = A\cos\left(M\Delta tn\right) + B\sin\left(M\Delta tn\right) + C$$

$$F_{(n-1)} = A\cos\left(M\Delta t\left(n-1\right)\right) + B\sin\left(M\Delta t\left(n-1\right)\right) + C$$

$$F_{(n-1)} = A\cos\left(M\Delta tn\right)\cos\left(M\Delta t\right) + A\sin\left(M\Delta tn\right)\sin\left(M\Delta t\right) + B\sin\left(M\Delta tn\right)\cos\left(M\Delta t\right) - B\cos\left(M\Delta tn\right)\sin\left(M\Delta t\right) + C$$

$$F_{(n-2)} = A\cos\left(M\Delta t\left(n-2\right)\right) + B\sin\left(M\Delta t\left(n-2\right)\right) + C$$

$$F_{(n-2)} = A\cos\left(M\Delta tn\right)\cos\left(2M\Delta t\right) + A\sin\left(M\Delta tn\right)\sin\left(2M\Delta t\right) + B\sin\left(M\Delta tn\right)\cos\left(2M\Delta t\right) - B\cos\left(M\Delta tn\right)\sin\left(2M\Delta t\right) + C$$

Substituting these functions in the equation we construct an algebraic system to obtain the coefficients as

$$\begin{bmatrix} k_1 \\ k_2 \\ k_3 \end{bmatrix} = \begin{bmatrix} a_{1,1} & a_{1,2} & a_{1,3} \\ a_{2,1} & a_{2,2} & a_{2,3} \\ a_{3,1} & a_{3,2} & a_{3,3} \end{bmatrix}^{-1} \begin{bmatrix} b_1 \\ b_2 \\ b_3 \end{bmatrix}$$

Where

$$a_{1,1} = D_1 + D_2\cos\left(M\Delta t\right) + D_3\cos\left(2M\Delta t\right)$$

$$a_{1,2} = -D_2\sin\left(M\Delta t\right) - D_3\sin\left(2M\Delta t\right)$$

$$a_{2,1} = D_2\sin\left(M\Delta t\right) + D_3\sin\left(2M\Delta t\right)$$

$$a_{2,2} = D_1 + D_2\cos\left(M\Delta t\right) + D_3\cos\left(2M\Delta t\right)$$

$$a_{1,3} = a_{2,3} = a_{3,1} = a_{3,2} = 0$$

$$a_{3,3} = D_1 + D_2 + D_3$$

And

$$b_1 = N_1A + N_2A\cos\left(M\Delta t\right) + N_3A\cos\left(2M\Delta t\right) - N_2B\sin\left(M\Delta t\right) - N_3B\sin\left(2M\Delta t\right)$$

$$b_2 = N_1B + N_2B\cos\left(M\Delta t\right) + N_3B\cos\left(2M\Delta t\right) + N_2A\sin\left(M\Delta t\right) + N_3A\sin\left(2M\Delta t\right)$$

$$b_3 = N_1C + N_2C + N_3C$$

solving the system, we arrive to

$$V_p\left(\mathrm{n}\right) = k_1\cos\left(M\Delta tn\right) + k_2\sin\left(M\Delta tn\right) + k_3$$

Homogeneous solution

The homogeneous solution is as follows

$$D_1V_n + D_2V_{(n-1)} + D_3V_{(n-2)} = 0$$

taking $\mathrm{V_n} = \mathrm{t^n}$ and substituting in the previous equation we obtain $D_1t^n + D_2t^{n-1} + D_3t^{n-2} = 0$ so $t^{n-2}\left(D_1t^2 + D_2t^1 + D_3t^0\right) = 0$

the solution of this equation yield to

$$V_h\left(n\right) = c_1r_1^n + c_2r_2^n$$

Finally we have

$$V\left(\mathrm{n}\right) = c_1r_1^n + c_2r_2^n + k_1\cos\left(M\Delta tn\right) + k_2\sin\left(M\Delta tn\right) + k_3$$

By using two solutions to generate a system to determine the unknown coefficients we obtain

$$V\left(0\right) = \mathrm{c_1r_1^0 + c_2r_2^0} + k_1\cos\left(M\Delta t\left(0\right)\right) + k_2\sin\left(M\Delta t\left(0\right)\right) + k_3$$

$$V\left(1\right) = \mathrm{c_1r_1^1 + c_2r_2^1} + k_1\cos\left(M\Delta t\left(1\right)\right) + k_2\sin\left(M\Delta t\left(1\right)\right) + k_3$$

Finally, we construct an algebraic system as

$$\begin{bmatrix} c_1 \\ c_2 \end{bmatrix} = \begin{bmatrix} r_1^0 & r_2^0 \\ r_1^1 & r_2^1 \end{bmatrix}^{-1} \begin{bmatrix} V\left(0\right) - k_1\cos\left(M\Delta t\left(0\right)\right) - k_2\sin\left(M\Delta t\left(0\right)\right) - k_3 \\ V\left(1\right) - k_1\cos\left(M\Delta t\left(1\right)\right) - k_2\sin\left(M\Delta t\left(1\right)\right) - k_3 \end{bmatrix}$$

The total solution is as follows

$$V\left(\mathrm{n}\right) = c_1r_1^n + c_2r_2^n + k_1\cos\left(M\Delta tn\right) + k_2\sin\left(M\Delta tn\right) + k_3$$

with $\mathrm{n} = 1:\mathrm{N}$ and $\mathrm{N} = \text{number of samples}$

Equation in differences solution from finite NEWTON differences

From the HOODE,

$$a_2\frac{d^2v}{dt^2} + a_1\frac{dv}{dt} + a_0v = A\cos\left(\omega\mathrm{t}\right) + B\sin\left(\omega\mathrm{t}\right) + C$$

we begin with the Newton differences as

$$\frac{d^2v}{dt^2} = \frac{V_n - 2V_{n-1} + V_{n-2}}{h^2}$$ and $$\frac{dv}{dt} = \frac{V_n - V_{n-1}}{h}$$

substituting into the equation we obtain

ISSN: 2410-3454.
RENIECYT-CONAHCYT: 1702902

Gutiérrez-Robles, José Alberto, Galván-Sánchez, Verónica Adriana, Bañuelos-Cabral, Eduardo Salvador and De La Cruz-García, Elba Lilia. Analysis of solution methods for high order ordinary differential equations used in electrical circuits. Journal of Engineering Applications. 2024. 11-32: 1-19
https://doi.org/10.35429/JEA.2024.32.11.1.19

$$a_2\left(\frac{V_n-2V_{n-1}+V_{n-2}}{h^2}\right)+a_1\left(\frac{V_n-V_{n-1}}{h}\right)+a_0V_n =$$
$$A\cos\left(M\Delta tn\right)+B\sin\left(M\Delta tn\right)+C$$

re-arranging we arrives to

$$\left(\frac{a_2}{h^2}+\frac{C_1}{h^1}+\frac{a_0}{h^0}\right)V_n+\left(-\frac{2a_2}{h^2}-\frac{a_1}{h^1}\right)V_{n-1}+\left(\frac{a_2}{h^2}\right)V_{n-2} =$$
$$A\cos\left(M\Delta tn\right)+B\sin\left(M\Delta tn\right)+C$$

or

$$Q_1V_n+Q_2V_{n-1}+Q_3V_{n-2} = A\cos\left(M\Delta tn\right)+B\sin\left(M\Delta tn\right)+C$$

Particular solution

Solving for the particular proposed solution, we obtain

$$V_n = k_1\cos\left(M\Delta tn\right)+k_2\sin\left(M\Delta tn\right)+k_3$$
$$V_{(n-1)} = k_1\cos\left(M\Delta t\left(n-1\right)\right)+k_2\sin\left(M\Delta t\left(n-1\right)\right)+k_3$$
$$V_{(n-1)} = k_1\cos\left(M\Delta tn\right)\cos\left(M\Delta t\right)+k_1\sin\left(M\Delta tn\right)\sin\left(M\Delta t\right)+$$
$$k_2\sin\left(M\Delta tn\right)\cos\left(M\Delta t\right)-k_2\cos\left(M\Delta tn\right)\sin\left(M\Delta t\right)+k_3$$
$$V_{(n-2)} = k_1\cos\left(M\Delta t\left(n-2\right)\right)+k_2\sin\left(M\Delta t\left(n-2\right)\right)+k_3$$
$$V_{(n-2)} = k_1\cos\left(M\Delta tn\right)\cos\left(2M\Delta t\right)+k_1\sin\left(M\Delta tn\right)\sin\left(2M\Delta t\right)+$$
$$k_2\sin\left(M\Delta tn\right)\cos\left(2M\Delta t\right)-k_2\cos\left(M\Delta tn\right)\sin\left(2M\Delta t\right)+k_3$$

Using these functions in the Newton difference equation we obtain a system like

$$\begin{bmatrix} k_1 \\ k_2 \\ k_3 \end{bmatrix} = \begin{bmatrix} a_{1,1} & a_{1,2} & a_{1,3} \\ a_{2,1} & a_{2,2} & a_{2,3} \\ a_{3,1} & a_{3,2} & a_{3,3} \end{bmatrix}^{-1} \begin{bmatrix} A \\ B \\ C \end{bmatrix}$$

where

$$a_{1,1} = Q_1+Q_2\cos\left(M\Delta t\right)+Q_3\cos\left(2M\Delta t\right)$$
$$a_{1,2} = -Q_2\sin\left(M\Delta t\right)-Q_3\sin\left(2M\Delta t\right)$$
$$a_{1,3} = 0$$
$$a_{2,1} = Q_2\sin\left(M\Delta t\right)+Q_3\sin\left(2M\Delta t\right)$$
$$a_{2,2} = Q_1+Q_2\cos\left(M\Delta t\right)+Q_3\cos\left(2M\Delta t\right)$$
$$a_{2,3} = a_{3,1} = a_{3,2} = 0$$

and $a_{3,3} = Q_1+Q_2+Q_3$

solving the system, we arrive to

$$V_p\left(\mathrm{n}\right) = k_1\cos\left(M\Delta tn\right)+k_2\sin\left(M\Delta tn\right)+k_3$$

Homogeneous solution

The homogeneous solution is as follows

$$Q_1V_n+Q_2V_{n-1}+Q_3V_{n-2} = 0$$

taking $V_n = t^n$ and substituting in the previous equation we obtain $Q_1t^n+Q_2t^{n-1}+Q_3t^{n-2}=0$ so $t^{n-2}\left(Q_1t^2+Q_2t^1+Q_3t^0\right)=0$ the solution of this equation yield to $V_h\left(\mathrm{n}\right)=c_1r_1^n+c_2r_2^n$

Finally we have

$$V\left(\mathrm{n}\right)=c_1r_1^n+c_2r_2^n+k_1\cos\left(M\Delta tn\right)+k_2\sin\left(M\Delta tn\right)+k_3$$

By using two solutions to generate a system to determine the unknown coefficients we obtain

$$V\left(0\right)=c_1r_1^0+c_2r_2^0+k_1\cos\left(M\Delta t\left(0\right)\right)+k_2\sin\left(M\Delta t\left(0\right)\right)+k_3$$
$$V\left(1\right)=c_1r_1^1+c_2r_2^1+k_1\cos\left(M\Delta t\left(1\right)\right)+k_2\sin\left(M\Delta t\left(1\right)\right)+k_3$$

Finally, we construct an algebraic system as

$$\begin{bmatrix} c_1 \\ c_2 \end{bmatrix} = \begin{bmatrix} r_1^0 & r_2^0 \\ r_1^1 & r_2^1 \end{bmatrix}^{-1} \begin{bmatrix} V\left(0\right)-k_1\cos\left(M\Delta t\left(0\right)\right)-k_2\sin\left(M\Delta t\left(0\right)\right)-k_3 \\ V\left(1\right)-k_1\cos\left(M\Delta t\left(1\right)\right)-k_2\sin\left(M\Delta t\left(1\right)\right)-k_3 \end{bmatrix}$$

The total solution is as follows

$$V\left(\mathrm{n}\right)=c_1r_1^n+c_2r_2^n+k_1\cos\left(M\Delta tn\right)+k_2\sin\left(M\Delta tn\right)+k_3$$

with $1\le n\le N \quad and \quad N = number\ of\ samples$

Solving with different Δt

Table 1 shows the used Δt in this equation, this table numbered each time step, for example the 20th position is associated with Δt equal to 0.4 seconds.

Box 1

Table 1

Position of each used Δt.

Pos	Δt in sec	Pos	Δt in sec	Pos	Δt in sec
1	2e-07	8	4e-05	15	0.008
2	4e-07	9	8e-05	16	0.02
3	8e-07	10	0.0002	17	0.04
4	2e-06	11	0.0004	18	0.08
5	4e-06	12	0.0008	19	0.2
6	8e-06	13	0.002	20	0.4
7	2e-05	14	0.004	21	0.8

Own generation

Note: We denote with green the Δt for which we obtain the lowest error and with blue the second Δt in term of the obtained error.

Lowest error for each kind of simulation
Next error for each kind of simulation

From table 2 to 17 we show all the made texts to the proposed ordinary differential equation.

ISSN: 2410-3454.
RENIECYT-CONAHCYT: 1702902

Gutiérrez-Robles, José Alberto, Galván-Sánchez, Verónica Adriana, Bañuelos-Cabral, Eduardo Salvador and De La Cruz-García, Elba Lilia. Analysis of solution methods for high order ordinary differential equations used in electrical circuits. Journal of Engineering Applications. 2024. 11-32: 1-19
https://doi.org/10.35429/JEA.2024.32.11.1.19

Box 2

Table 2

MSE taking the Laplace solution like a reference - $MSE_{Error} = abs(sum((Laplace - Method).^2))$/Ns

Δt in sec	Time domain	Z-domain	Differences from Z	Differences from Newton
2e-07	1.5921e-30	NaN	1.377e-09	1.2894e-12
4e-07	1.5921e-30	NaN	8.4146e-11	4.7858e-15
8e-07	1.5921e-30	NaN	1.922e-12	1.6928e-14
2e-06	1.5922e-30	NaN	1.9879e-12	1.0192e-12
4e-06	1.5922e-30	NaN	1.0566e-14	8.9919e-13
8e-06	1.5921e-30	NaN	6.0996e-16	3.9757e-12
2e-05	1.5924e-30	Inf	6.8982e-17	2.3767e-11
4e-05	1.5921e-30	6.77e+185	4.5111e-19	9.5358e-11
8e-05	1.5923e-30	2.221e+81	3.6698e-19	3.8149e-10
0.0002	1.5918e-30	8.143e+22	7.8259e-18	2.384e-09
0.0004	1.5919e-30	608.15	1.2763e-16	9.5336e-09
0.0008	1.5923e-30	0.0023425	2.0453e-15	3.8117e-08
0.002	1.5907e-30	7.1112e-06	7.989e-14	2.3789e-07
0.004	1.5916e-30	8.0817e-10	1.278e-12	9.4933e-07
0.008	1.5936e-30	1.6423e-09	2.0442e-11	3.7794e-06
0.02	1.5865e-30	6.3859e-08	7.9781e-10	2.3288e-05
0.04	1.5846e-30	1.021e-06	1.2749e-08	9.0959e-05
0.08	1.5896e-30	1.6222e-05	2.0369e-07	0.00034666
0.2	1.5795e-30	0.0005917	7.9807e-06	0.0018626
0.4	1.5696e-30	0.0071934	0.00013146	0.0056763
0.8	1.6396e-30	0.040308	0.0023949	0.013309

Own generation

Box 3

Table 3

Area Error taking the Laplace solution like a reference - $AREA_{Error} = abs(trapz(Laplace) - trapz(Method))$

Δt in sec	Time domain	Z-domain	Differences from Z	Differences from Newton
2e-07	3.3307e-15	NaN	5.8501e-05	4.6979e-06
4e-07	3.5527e-15	NaN	6.4537e-05	1.1724e-07
8e-07	3.5527e-15	NaN	3.5474e-06	4.1911e-07
2e-06	3.1086e-15	NaN	5.2728e-06	1.4228e-06
4e-06	3.5527e-15	Inf	5.8488e-07	1.8001e-06
8e-06	3.5527e-15	NaN	1.4061e-07	3.7146e-06
2e-05	3.5527e-15	1.16e+163	4.5574e-08	9.1643e-06
4e-05	3.3307e-15	6.213e+92	2.8457e-09	1.8345e-05
8e-05	3.5527e-15	4.944e+40	2.2008e-09	3.6691e-05
0.0002	3.3307e-15	5.674e+11	5.8192e-10	9.1725e-05
0.0004	3.5527e-15	105.86	2.4506e-09	0.00018344
0.0008	3.3307e-15	0.28607	1.0252e-08	0.00036683
0.002	3.5527e-15	0.016371	6.3911e-08	0.00091676
0.004	3.5527e-15	0.0001480	2.5434e-07	0.0018324
0.008	3.5527e-15	2.515e-05	1.007e-06	0.0036602
0.02	3.1086e-15	0.0001467	6.1051e-06	0.0091137
0.04	3.3307e-15	0.0005948	2.3251e-05	0.018088
0.08	3.5527e-15	0.0024562	8.4909e-05	0.035502
0.2	3.3307e-15	0.01734	0.00043589	0.081493
0.4	3.1086e-15	0.080994	0.0016637	0.12587
0.8	3.1086e-15	0.20659	0.0079006	0.038226

Own generation

Box 4

Table 4

Percent Error taking the Laplace solution like a reference
$\%_{Error} = abs(sum((Lap - Method)/max(Lap)))$/Ns

Δt in sec	Time domain	Z-domain	Differences from Z	Differences from Newton
2e-07	1.0409e-15	NaN	1.7834e-05	1.4321e-06
4e-07	1.0409e-15	NaN	1.9674e-05	3.5739e-08
8e-07	1.041e-15	NaN	1.0814e-06	1.2776e-07
2e-06	1.041e-15	NaN	1.6074e-06	4.3374e-07
4e-06	1.041e-15	Inf	1.783e-07	5.4876e-07
8e-06	1.0409e-15	NaN	4.2865e-08	1.1324e-06
2e-05	1.041e-15	3.55e+162	1.3893e-08	2.7937e-06
4e-05	1.0409e-15	1.895e+92	8.6749e-10	5.5924e-06
8e-05	1.0405e-15	1.506e+40	6.7092e-10	1.1185e-05
0.0002	1.0413e-15	1.730e+11	1.7746e-10	2.7963e-05
0.0004	1.0403e-15	32.275	7.4757e-10	5.5924e-05
0.0008	1.0404e-15	0.087199	3.1292e-09	0.00011184
0.002	1.0383e-15	0.0049899	1.9546e-08	0.00027957
0.004	1.0392e-15	4.5089e-05	7.804e-08	0.000559
0.008	1.0394e-15	7.528e-06	3.1101e-07	0.0011174
0.02	1.0277e-15	4.2586e-05	1.9243e-06	0.0027881
0.04	1.0186e-15	0.0001643	7.5938e-06	0.0055527
0.08	1.0132e-15	0.0006169	2.9947e-05	0.010978
0.2	9.6246e-16	0.0034557	0.00019556	0.025719
0.4	8.7295e-16	0.015162	0.0010144	0.043009
0.8	7.1562e-16	0.059835	0.0057003	0.029467

Own generation

NOTE: The results that are highlighted are those with the lowest error for each presented method.

Box 5

Table 5

MSE using f=60 Hz
$MSE_{Error} = abs(sum((Laplace - Method).^2))$/Ns

Method	Time domain	Z-domain	Differences from Z	Differences Newton
Error	6.1124e-33	3.5386e-10	2.9712e-17	4.245e-14
Position	15	15	7	4
Error	6.1493e-33	4.0871e-10	1.1584e-16	5.5324e-14
Position	13	16	8	2

Own generation

Box 6

Table 6

Area Error using f=60 Hz
$$AREA_{Error} = abs(trapz(Laplace) - trapz(Method))$$

Method	Time domain	Z-domain	Differences from Z	Differences Newton
Error	4.4409e-16	8.5023e-08	2.6795e-08	7.7232e-07
Position	15	14	7	4
Error	4.4409e-16	1.1263e-07	3.9154e-08	1.0162e-06
Position	18	15	8	2

Own generation

ISSN: 2410-3454.
RENIECYT-CONAHCYT: 1702902

Journal of Engineering Applications December 2024 Vol.11 No.32 1-19
Article

Box 7

Table 7

Percent Error using f=60 Hz

$\%_{Error} = abs(sum((Lap - Method)/max(Lap)))/Ns$

Method	Time domain	Z-domain	Differences from Z	Differences Newton
Error	5.8716e-16	6.3457e-08	2.679e-08	7.7216e-07
Position	15	14	7	4
Error	5.8937e-16	6.8251e-08	3.9146e-08	1.016e-06
Position	13	15	8	2

Own generation

Box 8

Table 8

MSE using A=2e20, B=3e20 and C=1e20 - $MSE_{Error} = abs(sum((Laplace - Method).^2))/Ns$

Method	Time domain	Z-domain	Differences from Z	Differences Newton
Error	1.6838e+10	8.0817e+30	3.6698e+21	4.7858e+25
Position	13	14	9	2
Error	1.6838e+10	1.6423e+31	4.5111e+21	1.6928e+26
Position	15	15	8	3

Box 9

Table 9

Area Error using A=2e20, B=3e20 and C=1e20 - $AREA_{Error} = abs(trapz(Laplace) - trapz(Method))$

Method	Time domain	Z-domain	Differences from Z	Differences Newton
Error	3.2768e+05	2.515e+15	5.8189e+10	1.1724e+13
Position	2	15	10	2
Error	3.2768e+05	1.4674e+16	2.2008e+11	4.1911e+13
Position	6	16	9	3

Box 10

Table 10

Percent Error using A=2e20, B=3e20 and C=1e20 - $\%_{Error} = abs(sum((Lap - Method)/max(Lap)))/Ns$

Method	Time domain	Z-domain	Differences from Z	Differences Newton
Error	7.9708e-16	7.528e-06	1.7745e-10	3.574e-08
Position	21	15	10	2
Error	9.3418e-16	4.2586e-05	6.7091e-10	1.2776e-07
Position	20	16	9	3

Box 11

Table 11

MSE with A=2e20, B=3e20, C=1e20 and F=60 Hz

$MSE_{Error} = abs(sum((Laplace - Method).^2))/Ns$

Method	Time domain	Z-domain	Differences from Z	Differences Newton
Error	5.8712e+07	3.5386e+30	2.9712e+23	4.245e+26
Position	16	15	7	4
Error	5.9091e+07	4.0871e+30	1.1584e+24	5.5325e+26
Position	17	16	8	2

Box 12

Table 12

Area Error using A=2e20, B=3e20, C=1e20 and F=60 Hz

$AREA_{Error} = abs(trapz(Laplace) - trapz(Method))$

Method	Time domain	Z-domain	Differences from Z	Differences Newton
Error	49152	8.5023e+12	2.6795e+12	7.7232e+13
Position	1	14	7	4
Error	49152	1.1263e+13	3.9154e+12	1.0162e+14
Position	4	15	8	2

Box

Table 13

Percent Error A=2e20, B=3e20, C=1e20 and F=60 Hz

$\%_{Error} = abs(sum((Lap - Method)/max(Lap)))/Ns$

Method	Time domain	Z-domain	Differences from Z	Differences Newton
Error	5.7701e-16	6.3457e-08	2.679e-08	7.7216e-07
Position	16	14	7	4
Error	5.7985e-16	6.8251e-08	3.9146e-08	1.016e-06
Position	17	15	8	2

Box 14

Table 14

Errors using different values for A, B, C and F

A=2, B=3, C=1 and F=1/pi Hz.

Kind of error	Time domain	Z-domain	Differences from Z	Differences Newton
RMS_{Error}	20	14	9	2
	19	15	8	3
$AREA_{Erro}$	20	15	10	2
	4	16	9	3
$\%_{Error}$	21	15	10	2
	20	16	9	3

Box 15

Table 15

Errors using different values for A, B, C and F

A=2, B=3, C=1 and F=60 Hz.

Kind of error	Time domain	Z-domain	Differences from Z	Differences Newton
RMS_{Error}	15	15	7	4
	13	16	8	2
$AREA_{Erro}$	15	14	7	4
	18	15	8	2
$\%_{Error}$	15	14	9	2
	13	15	8	3

Box 16

Table 16

Errors using different values for A, B, C and F

A=2e20, B=3e20, C=1e20 and F=1/pi Hz.

Kind of error	Time domain	Z-domain	Differences from Z	Differences from Newton
RMS_{Error}	13	14	9	2
	15	15	8	3
$AREA_{Erro}$	2	15	10	2
	6	16	9	3
$\%_{Error}$	21	15	10	2
	20	16	9	3

ISSN: 2410-3454.
RENIECYT-CONAHCYT: 1702902

Box 17

Table 17

Errors using different values for A, B, C and F
A=2e20, B=3e20, C=1e20 and F=60 Hz.

Kind of error	Time domain	Z-domain	Differences from Z	Differences from Newton
RMS_{Error}	16	15	7	4
	17	16	8	2
$AREA_{Erro}$	1	14	7	4
	4	15	8	2
$\%_{Error}$	16	14	7	4
	17	15	8	2

Findings

Errors are calculated according to the equation shown in the header of each table. In the case of MSE, the difference between samples is calculated, squared and added; For the case of area error, the area under the curve is calculated with the trapezoidal rule and the absolute difference is obtained. Thus, analyzing the results obtained, the following was found:

1. The solution in time compared to Laplace are practically identical, the differences are due to the fact that numerical computation in binary is of finite length and therefore has an inherent error.

2. The foregoing is noticeable when seeing the RMS error in which it decreases because as the delta t increases, the samples decrease, but the area error is correspondingly similar for all cases.

3. The Z transform depends on the delta t used, so for the case of a very small delta t the methodology is indeterminate, as the delta t grows it stabilizes numerically until it reaches its maximum precision, then as the delta t increases it loses precision.

4. The difference equation, starting from the Z transform, increases precision as delta t grows until it reaches a point where more and more precision is lost.

If all the results are analyzed, it is concluded that, at least for this equation, there is no delta t that is suitable for all implementations. Figure 1 and 2 shows graphically one of these results.

Box 18

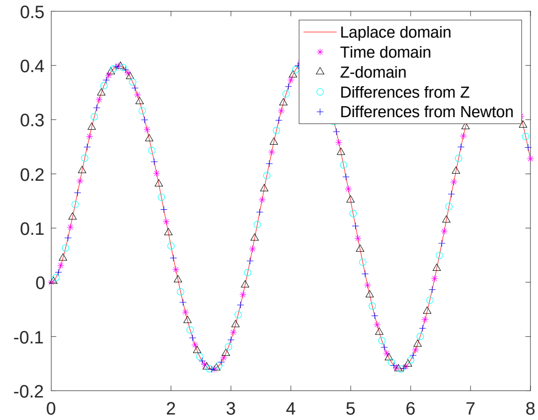

Figure 1
Solution by using A=2, B=3, C=1 and F=1/pi Hz

Box 19

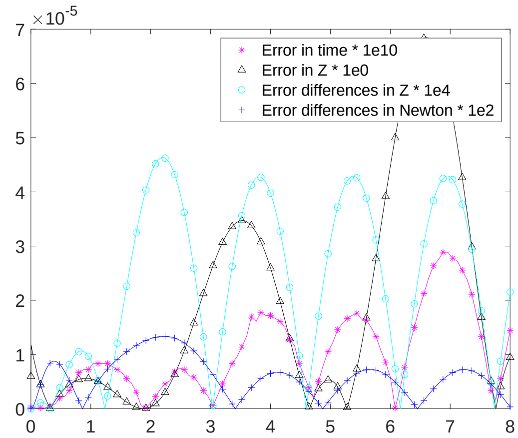

Figure 2
Error by using A=2, B=3, C=1 and F=1/pi Hz

Second example

This example (figure 3) is constructed from the roots, that means, the exact solution of the representative polynomial is known a priori, for that reason it is possible to construct the analytical solution in exact form. The HOODE is,

$$\frac{d^3v}{dt^3}+C\frac{d^2v}{dt^2}+D\frac{dv}{dt}+Ev=A\cos(\omega t)+B\sin(\omega t)+C$$

with $C=200$, $D=4040004$, $E=40000$, $A=-10000w^2$, $B=-2000000w$, $C=0$ and $T_{obs}=4$ seconds. The initial conditions, $v=0$, $v'=0$ and $v''=0$

Gutiérrez-Robles, José Alberto, Galván-Sánchez, Verónica Adriana, Bañuelos-Cabral, Eduardo Salvador and De La Cruz-García, Elba Lilia. Analysis of solution methods for high order ordinary differential equations used in electrical circuits. Journal of Engineering Applications. 2024. 11-32: 1-19
https://doi.org/10.35429/JEA.2024.32.11.1.19

Box 20

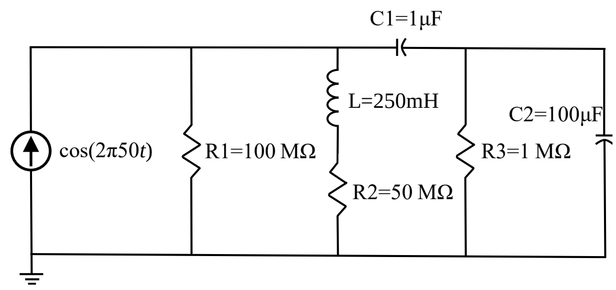

Figure 3
Electrical network used in this example

Using the Laplace transforms

Applying the Laplace to the HOODE and taking into account the initial conditions, one obtains:

$$s^3+Cs^2+Ds+E=\frac{As}{s^2+\omega^2}+\frac{B\omega}{s^2+\omega^2}$$

So, the transfer function is,

$$H(s)=\frac{As+B\omega}{s^5+k_1s^4+k_2s^3+k_3s^2+k_4s+k_5}$$

with $k_1=200$, $k_2=4182126$, $k_3=28464460$, $k_4=574174674126$, and $k_5=5684892135$.

Decomposing in partial fractions and solved we obtain

$$H(s)=\frac{-0.0182-0.0889i}{s+(-99.99+2007.48i)}+\frac{-0.0182+0.0889i}{s+(-99.99-2007.48i)}+\frac{-0.4950}{s+(-0.0099)}+\frac{0.2657+0.4784i}{s-376.99i}+\frac{0.2657-0.4784i}{s+376.99i}$$

Finally in time domain, with $r_1=-99.9950+2007.4867i$, $r_2=-99.9950-2007.4867i$ and $r_3=-0.0099$, we have

$$v(t)=(-0.0182-0.0889i)e^{-r_1t}+(-0.0182+0.0889i)e^{-r_2t}+(-0.4950)e^{-r_3t}+2e^{-0t}\left(0.265791\cos(\omega t)-0.478450\sin(\omega t)\right)$$

Time domain solution

The HOODE is,

$$\frac{d^3v}{dt^3}+C\frac{d^2v}{dt^2}+D\frac{dv}{dt}+Ev=A\cos(\omega t)+B\sin(\omega t)$$

The proposed solution in time domain is as follows,

$$v_T(t)=c_1e^{-r_1t}+c_2e^{-r_2t}+c_3e^{-r_3t}+b_1\cos(\omega t)+b_2\sin(\omega t)$$

Time domain particular solution

The particular proposed solution is as follows,

$$v_p(t)=b_1\cos(\omega t)+b_2\sin(\omega t)$$

which solution yield to

$$v_p(t)=0.53158\cos(\omega t)-0.9569\sin(\omega t)$$

Time domain homogenous solution

Using this solution, we have the total solution as:

$$v_T(t)=c_1e^{-r_1t}+c_2e^{-r_2t}+c_3e^{-r_3t}+0.5315\cos(\omega t)-0.9569\,\mathrm{sen}(\omega t)$$

by using this proposed solution with $r_1=-99.99+2007.5i$, $r_2=-99.99-2007.5i$, $r_3=-0.0099$, and the initial conditions, to generate the algebraic system, we obtain: $c_1=-0.0182-0.0889$, $c_1=-0.0182+0.0889$ and $c_3=-0.4950$; so, the final solution is,

$$v_T(t)=(-0.0182-0.0889)e^{-r_1t}+(-0.0182+0.0889)e^{-r_2t}-0.4950e^{-r_3t}+0.5315\cos(\omega t)-0.9569\sin(\omega t)$$

Z-transform solution

The solution in z-plane is constructed from $H(s)$, so we have

$$H(s)=\frac{As+B\omega}{s^5+k_1s^4+k_2s^3+k_3s^2+k_4s+k_5}$$

Then, by using MatLab to construct Hz; first it is used the instruction "Hs=tf([Ns], [Ds])" which creates a continuous-time transfer function SYS as,

- Hs=tf([A w*B], [k_1 k_2 k_3 k_4 k_5])

Having Hs, we use c2d to compute a discrete time model Hz, with sample time $h=8x10^{-5}$, and with the trapezoidal rule that approximates the continuous time model.

- Hz = c2d(Hs,h,'tustin')

So, we have

$$H(z)=\frac{W(z)}{F(z)}=\frac{-3.61e^{-9}z^5-1.09e^{-8}z^4-7.45e^{-9}z^3+6.88e^{-9}z^2+1.06e^{-8}z+3.55e^{-9}}{z^5-4.958z^4+9.858z^3-9.826z^2+4.911z-0.9842}$$

Finally, we use the function "residuez" to find the z-transform partial-fraction expansion of N(z)/D(z), so we obtain the residues, poles and direct term as [r,p,Kp]=residuez(Hz.Numerator{1}, Hz.Denominator{1})

ISSN: 2410-3454.
RENIECYT-CONAHCYT: 1702902

Gutiérrez-Robles, José Alberto, Galván-Sánchez, Verónica Adriana, Bañuelos-Cabral, Eduardo Salvador and De La Cruz-García, Elba Lilia. Analysis of solution methods for high order ordinary differential equations used in electrical circuits. Journal of Engineering Applications. 2024. 11-32: 1-19
https://doi.org/10.35429/JEA.2024.32.11.1.19

We construct the solution of the HOODE in z-domain as,

$$v(t)=\frac{r_1(p_1)^{ke}+r_2(p_2)^{ke}+r_3(p_3)^{ke}+r_4(p_4)^{ke}+r_5(p_5)^{ke}}{h}$$

with $r_1=2.125e^{-5}+3.826e^{-5}i$, $r_2=2.125e^{-5}-3.826e^{-5}i$, $r_3=-3.960e^{-5}$, $r_4=-1.457e^{-6}-7.068e^{-6}i$, $r_5=-1.457e^{-6}+7.068e^{-6}i$, $p_1=0.999+0.030$, $p_2=0.999-0.030$, $p_3=1$, $p_4=0.979+0.158$, $p_5=0.979-0.158$, $Kp=0$, $1\le ke\le n-1$, and $\text{n}=\text{number of samples}$. The first sample is corrected with the direct term as, $v(1)=v(1)+\frac{Kp}{h}$.

Equation in differences solution from z

The solution begins with the transfer function of the left side of the differential equation, so we have

$$H(s)=\frac{1}{s^3+200s^2+4040004s+40000}$$

by using $\text{H}(\text{s})$ with $\text{h}=4\text{x}10^{-6}$, in z-domain we obtain

$$H(z)=\frac{V(z)}{F(z)}$$

$$=\frac{\left[7.997e^{-18}z^3+2.399e^{-17}z^2+2.399e^{-17}z+7.997e^{-18}\right]}{\left[z^3-2.999z^2+2.998z-0.999\right]}\frac{z^{-3}}{z^{-3}}$$

that is

$$H(z)=\frac{V(z)}{\text{F}(z)}=\frac{\left[N_1+N_2z^{-1}+N_3z^{-2}+N_4z^{-3}\right]}{\left[D_1+D_2z^{-1}+D_3z^{-2}+D_4z^{-3}\right]}$$

Re-arranging we arrive to

$$V(z)\left[D_1+D_2z^{-1}+D_3z^{-2}+D_4z^{-3}\right]=F(z)\left[N_1+N_2z^{-1}+N_3z^{-2}+N_4z^{-3}\right]$$

So we have

$$D_1V_n+D_2V_{(n-1)}+D_3V_{(n-2)}+D_4V_{(n-3)}=N_1F_n+N_2F_{(n-1)}+N_3F_{(n-2)}+N_4F_{(n-3)}$$

Particular solution

Solving for the particular proposed solution, we obtain

$$V_n=k_1\cos(M\Delta tn)+k_2\sin(M\Delta tn)+k_3$$
$$V_{(n-1)}=k_1\cos(M\Delta t(n-1))+k_2\sin(M\Delta t(n-1))+k_3$$
$$V_{(n-2)}=k_1\cos(M\Delta t(n-2))+k_2\sin(M\Delta t(n-2))+k_3$$

and

$$F_n=A\cos(M\Delta tn)+B\sin(M\Delta tn)+C$$
$$F_{(n-1)}=A\cos(M\Delta t(n-1))+B\sin(M\Delta t(n-1))+C$$
$$F_{(n-2)}=A\cos(M\Delta t(n-2))+B\sin(M\Delta t(n-2))+C$$

Substituting these functions in the equation we construct an algebraic system to obtain the coefficients. So, we arrive to

$$V_p(n)=0.53158\cos(M\Delta tn)-0.9569\sin(M\Delta tn)$$

Homogeneous solution

The homogeneous solution is as follows

$$D_1V_n+D_2V_{(n-1)}+D_3V_{(n-2)}+D_4V_{(n-3)}=0$$

taking and substituting in the previous equation we obtain

$$D_1t^n+D_2t^{n-1}+D_3t^{n-2}+D_4t^{n-3}=0$$

so

$$t^{n-3}\left(D_1t^3+D_2t^2+D_3t^1+D_4t^0\right)=0$$

the solution of this equation yield to

$$V_h(n)=c_1r_1^n+c_2r_2^n+c_3r_3^n$$

with $r_1=-99.9950+2007.4867$, $r_2=-99.9950-2007.4867$ and $r_3=\text{-}\,0.0099$.

Finally, we have

$$V(n)=c_1r_1^n+c_2r_2^n+c_3r_3^n$$
$$+0.53158\cos(M\Delta tn)-0.9569\sin(M\Delta tn)$$

By using three solutions to generate a system to determine the unknown coefficients we obtain

$$V(n)=(-0.018279-0.088938i)r_1^n+(-0.018279+0.088938i)r_2^n$$
$$-0.49502r_3^n+0.53158\cos(M\Delta tn)-0.9569\sin(M\Delta tn)$$

with $\text{n}=1:\text{N}$ and $\text{N}=\text{number of samples}$

Equation in differences solution from finite Newton differences

From the HOODE,

$$a_3\frac{d^3v}{dt^3}+a_2\frac{d^2v}{dt^2}+a_1\frac{dv}{dt}+a_0v=A\cos(\omega\text{t})+B\sin(\omega\text{t})$$

substituting into the equation Newton difference, with $\text{h}=8\text{x}10^{-7}$, we obtain

$$Q_1V_n+Q_2V_{n-1}+Q_3V_{n-2}+Q_4V_{n-3}=A\cos(M\Delta tn)+B\sin(M\Delta tn)$$

with

$$Q_1=1953442550005040128$$
$$Q_2=-5860005050005001216$$

ISSN: 2410-3454.
RENIECYT-CONAHCYT: 1702902

$Q_3 = 5859687500000001024$ and
$Q_4 = -1953125000000000256$

Particular solution

Solving for the particular proposed solution, we obtain
$$V_n = k_1 \cos(M\Delta tn) + k_2 \sin(M\Delta tn)$$

Using these functions in the Newton difference equation we arrive to
$$V_p(\mathrm{n}) = \frac{2780}{5231}\cos(M\Delta tn) - \frac{645}{674}\sin(M\Delta tn)$$

Homogeneous solution

The homogeneous solution is as follows
$$Q_1V_n + Q_2V_{n-1} + Q_3V_{n-2} + Q_4V_{n-3} = 0$$
taking $\mathrm{V_n} = \mathrm{t^n}$ and substituting in the previous equation we obtain
$$Q_1t^n + Q_2t^{n-1} + Q_3t^{n-2} + Q_4t^{n-3} = 0$$

so
$$t^{n-3}\left(Q_1t^3 + Q_2t^2 + Q_3t^1 + Q_4t^0\right) = 0$$

the solution of this equation yield to
$$V_h(n) = c_1\left(\frac{12110}{12111} + \frac{74}{46085}i\right)^n + c_2\left(\frac{12110}{12111} - \frac{74}{46085}i\right)^n + c_3(1)^n$$

Finally we have
$$V(n) = c_1r_1^n + c_2r_2^n + c_3r_3^n + \frac{2780}{5231}\cos(M\Delta tn) - \frac{645}{674}\sin(M\Delta tn)$$

By using two solutions to generate a system to determine the unknown coefficients we obtain the solution as follows
$$V(n) = \left(-\frac{39}{2117} - \frac{290}{3261}i\right)\left(\frac{12110}{12111} + \frac{74}{46085}i\right)^n + \left(-\frac{39}{2117} + \frac{290}{3261}i\right)\left(\frac{12110}{12111} - \frac{74}{46085}i\right)^n - \frac{504}{1019}(1)^n + \frac{2780}{5231}\cos(M\Delta tn) - \frac{645}{674}\sin(M\Delta tn)$$

with $\mathrm{n} = 1:\mathrm{N}$ and $\mathrm{N} = \text{number of samples}$

Figure 4 and 5 show the solution for some specific values by using all methods, while figure 4 shows the resulting solution, figure 5 shows the errors taking the Laplace method like a reference.

Box 21

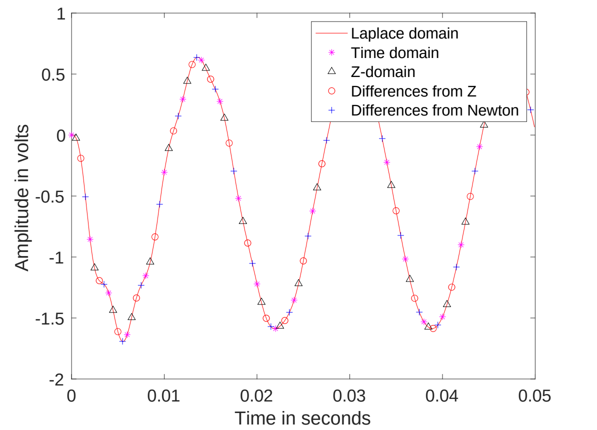

Figure 4
Solution by using A=2, B=3, C=1 and F=1/pi Hz

Box 22

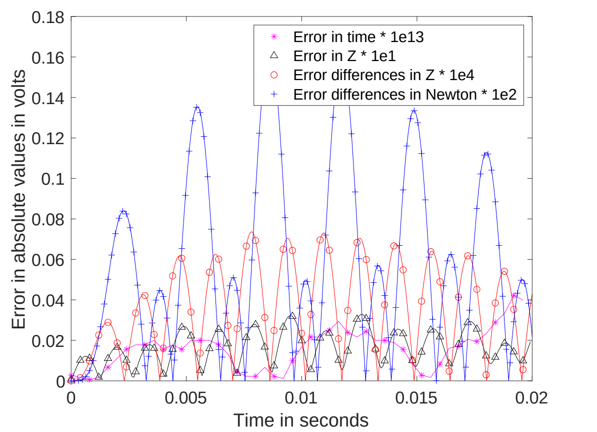

Figure 5
Error taking Laplace like a reference

Table 18 shows the solution for each method, this table only shows the two times steps for which we obtain the best solutions and/or the lowest errors.

Box 23

Table 18
Errors using different values for A, B, C and F
A=-1e4*w^2, B=-2e6*w, C=0 and F=60 Hz.

Kind of error	Time domain	Z-domain	Differences from Z	Differences Newton
MSE_{Error}	4.7435e-26	0.0082716	9.1915e-13	2.2021e-07
	19	9	5	3
	4.7794e-26	0.09869	2.786e-12	1.2037e-06
	12	10	6	4
$AREA_{Erro}$	4.6567e-19	0.02863	2.9443e-06	0.0018132
	8	18	6	3
	2.2205e-16	0.034245	3.2246e-06	0.0042225
	9	17	5	4
$\%_{Error}$	1.1081e-17	0.015567	1.1536e-06	0.00071045
	10	12	6	3
	9.9914e-17	0.017007	1.2635e-06	0.0016545
	12	15	5	4

ISSN: 2410-3454.
RENIECYT-CONAHCYT: 1702902

Gutiérrez-Robles, José Alberto, Galván-Sánchez, Verónica Adriana, Bañuelos-Cabral, Eduardo Salvador and De La Cruz-García, Elba Lilia. Analysis of solution methods for high order ordinary differential equations used in electrical circuits. Journal of Engineering Applications. 2024. 11-32: 1-19
https://doi.org/10.35429/JEA.2024.32.11.1.19

Third example

The circuit in figure 6 is a classic example of a □-cascade that can come from the adjustment of a line, for this case fictitious values were used to show the HOODE methods. The circuit begging in repose conditions, means, the inductors and capacitors are discharged.

Box 24

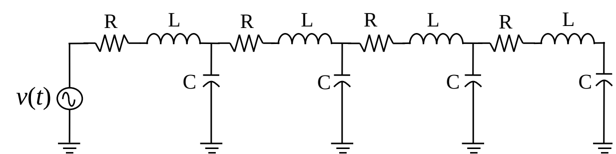

Figure 6

Electrical circuit with R=2 Ω, L=0.5 H and C=0.1 F

The first step is to obtain the transfer function or high-order equation that defines the circuit, this is obtained by analyzing the circuit and is the following:

$$\frac{d^8v}{dt^8}+16\frac{d^7v}{dt^7}+236\frac{d^6v}{dt^6}+1936\frac{d^5v}{dt^5}+12976\frac{d^4v}{dt^4}+56960\frac{d^3v}{dt^3}+$$
$$176000\frac{d^2v}{dt^2}+320000\frac{dv}{dt}+160000=160000\sin(t)$$

This equation has the following roots:

$r_1=-2+8.1634i, r_2=-2-8.1634i, r_3=-2+6.5533i$
$r_4=-2-6.5533i, r_5=-2+4i, r_6=-2-4i, r_7=-3.26$
and $r_8=-0.73996$; so, with initial conditions equal to zero, the solution is as follows.

Using the Laplace transform

The analytical solution can be obtained by two different methods, the one with indeterminate coefficients or using the Laplace transform, regardless of which one is used, the solution obtained is:

$$\begin{aligned} v(t) = {} & 2\,\mathrm{e}^{-2t}\left[-0.0008\cos(8.1634t)+0.0015\,\mathrm{sen}(8.1634t)\right] \\ & +2\,\mathrm{e}^{-2t}\left[0.0053\cos(6.5533t)-0.0077\,\mathrm{sen}(6.5533t)\right] \\ & +2\,\mathrm{e}^{-2t}\left[-0.0354\cos(4t)+0.0243\,\mathrm{sen}(4t)\right] \\ & -0.1022\,\mathrm{e}^{-3.26t}+0.7677\,\mathrm{e}^{-0.74t} \\ & +2\left[-0.3019\cos(t)-0.0037\,\mathrm{sen}(t)\right] \end{aligned}$$

Time domain solution

The proposed solution in time domain is as follows,

$$v_T(t)=c_1e^{-r_1t}+c_2e^{-r_2t}+c_3e^{-r_3t}+c_4e^{-r_4t}+c_5e^{-r_5t}+c_6e^{-r_6t}$$
$$+c_7e^{-r_7t}+c_8e^{-r_8t}+b_1\cos(\omega t)+b_2\sin(\omega t)$$

Time domain particular solution

The particular proposed solution is as follows,
$$v_p(t)=b_1\cos(\omega t)+b_2\sin(\omega t)$$
which solution yield to
$$v_p(t)=-0.60377\cos(\omega t)-0.0074264\sin(\omega t)$$

Time domain homogenous solution

Using this solution, we have the total solution as:

$$\begin{aligned} v_T(t) = {} & c_1e^{-r_1t}+c_2e^{-r_2t}+c_3e^{-r_3t}+c_4e^{-r_4t}+c_5e^{-r_5t} \\ & +c_6e^{-r_6t}+c_7e^{-r_7t}+c_8e^{-r_8t} \\ & -0.60377\cos(\omega t)-0.0074264\sin(\omega t) \end{aligned}$$

by using this proposed solution with $r_1=-2+8.1634i$, $r_2=-2-8.1634i$, $r_3=-2+6.5533i$, $r_4=-2-6.5533i$, $r_5=-2+4i$, $r_6=-2-4i$, $r_7=-3.26$, $r_8=-0.73996$, and the initial conditions, to generate the algebraic system, the final solution is,

$$\begin{aligned} \mathrm{v_T}(\mathrm{t}) = {} & (-0.0008-0.0015i)e^{-r_1t}+(-0.0008-0.0015i)e^{-r_2t} \\ & +(0.0052+0.0076i)e^{-r_3t}+(0.0052-0.0076i)^{-r_4t} \\ & +(-0.0353-0.0243i)e^{-r_5t}+(-0.0353+0.0243i)e^{-r_6t} \\ & -0.10217e^{-r_7t}+0.7677e^{-r_8t} \\ & -0.60377\cos(\omega \mathrm{t})-0.0074264\sin(\omega \mathrm{t}) \end{aligned}$$

Z-transform solution

The first step to obtain the solution using the z-transform technique is to obtain the transfer function in *z* from the function in *s*, with $h=8x10^{-2}$, from here we obtain:

$$V(z)=\frac{\begin{gathered}7.679\mathrm{x}10^{-10}z^{10}+7.679\mathrm{x}10^{-9}z^9+3.456\mathrm{x}10^{-8}z^8+\\9.215\mathrm{x}10^{-8}z^7+1.613\mathrm{x}10^{-7}z^6+1.935\mathrm{x}10^{-7}z^5+1.613\mathrm{x}10^{-7}z^4+\\9.215\mathrm{x}10^{-8}z^3+3.456\mathrm{x}10^{-8}z^2+7.679\mathrm{x}10^{-9}z+7.679\mathrm{x}10^{-10}\end{gathered}}{\begin{gathered}z^{10}-8.221z^9+30.87z^8-69.8z^7+105.2z^6-110.7z^5+\\82.19z^4-42.59z^3+14.74z^2-3.077z+0.2942\end{gathered}}$$

The previous function is expanded in partial fractions to obtain the residues (*R*), the poles (*P*), and the constant of proportionality (*kp*), from which, we obtain:

ISSN: 2410-3454.
RENIECYT-CONAHCYT: 1702902

$$R=\begin{bmatrix}-0.024112+0.00029654i\\-0.024112-0.00029654i\\0.061471\\-6.3495e-05-0.00010723i\\-6.3495e-05+0.00010723i\\0.00042055+0.00056017i\\0.00042055-0.00056017i\\-0.0028222-0.0018376i\\-0.0028222+0.0018376i\\-0.0083152\end{bmatrix},\quad P=\begin{bmatrix}0.99681+0.079872i\\0.99681-0.079872i\\0.94251\\0.69674+0.51301i\\0.69674-0.51301i\\0.74883+0.42447i\\0.74883-0.42447i\\0.81208+0.26846i\\0.81208-0.26846i\\0.76928\end{bmatrix},$$

$kp=2.6101x10^{-9}$ *and* $h=8x10^{-2}$

with these data the solution of the differential equation is formed as $v(t)=sum(R.'\ P^n)$, where n is the sample number and $(.')$ means a vector operation element by element; the first sample must be corrected with the constant of proportionality with $v(1)=v(1)+kp/h$.

Equation in differences solution from z

When doing the process of having a difference equation starting from the z transform, with $h=2x10^{-2}$,the following expression is reached,

$$\begin{aligned}&v(n-0)-7.6398v(n-1)+25.58v(n-2)-49.03v(n-3)+58.84v(n-4)\\&-45.272v(n-5)+21.809v(n-6)-6.0139v(n-7)+0.72684v(n-8)\\&=8.434x10^{-17}\sin((n-0)h)+6.7472x10^{-16}\sin((n-1)h)\\&+2.3615x10^{-15}\sin((n-2)h)+4.7231x10^{-15}\sin((n-3)h)\\&+5.9038x10^{-15}\sin((n-4)h)+4.7231x10^{-15}\sin((n-5)h)\\&+2.3615x10^{-15}\sin((n-6)h)+6.7472x10^{-16}\sin((n-7)h)\\&+8.434x10^{-17}\sin((n-8)h)\end{aligned}$$

Reducing the right part of the equation with the identity

$A\sin(n-k)=A\sin(n)\cos(k)-A\cos(n)\sin(k)$

we obtain,

$$\begin{aligned}&v(n-0)-7.6398v(n-1)+25.58v(n-2)\\&-49.03v(n-3)+58.84v(n-4)-45.272v(n-5)\\&+21.809v(n-6)-6.0139v(n-7)+0.72684v(n-8)\\&=-2.7596x10^{-10}\cos(nh)+3.4422x10^{-9}\sin(nh)\end{aligned}$$

The solution to this equation leads to

$$v(t)=\text{sum}(R.\times P^n)-0.60376\cos(nh)-0.0074491\sin(nh)$$

with

$$R=\begin{bmatrix}-0.00080109-0.0015378i\\-0.0008011+0.0015378i\\0.0052847+0.0077361i\\0.0052847-0.007736i\\-0.03536-0.024464i\\-0.03536+0.024464i\\0.76748\\-0.10196\end{bmatrix},P=\begin{bmatrix}0.9483+0.15593i\\0.9483-0.15593i\\0.95272+0.12546i\\0.95272-0.12546i\\0.95777+0.076776i\\0.95777-0.076776i\\0.98531\\0.93686\end{bmatrix}$$

and $h=2x10^{-2}$

Equation in differences solution from finite Newton differences

The direct implementation of the high-order differential equation in finite differences is unstable, so we proceeded to obtain the difference equation from which the coefficients and roots were obtained, with $h=8x10^{-2}$

$$R=\begin{bmatrix}-0.00087625-0.0016603i\\-0.0008768+0.0016592i\\0.0055132+0.0081145i\\0.0055127-0.0081064i\\-0.036124-0.025104i\\-0.036126+0.025101i\\0.76761\\-0.10348\end{bmatrix},\quad P=\begin{bmatrix}0.9802+0.062997i\\0.9802-0.062997i\\0.98164+0.050687i\\0.98164-0.050687i\\0.98327+0.030904i\\0.98327-0.030904i\\0.99402\\0.97468\end{bmatrix}$$

and $h=8x10^{-2}$

So, the solution is obtained as,

$$v(t)=\text{sum}(R.\times P^n)+-0.60376\cos(nh)-0.0074491\sin(nh)$$

Analyzing the absolute values of the roots of the difference equation, these are greater than unity and therefore the solution is unstable, for this reason it is not included in the simulation results.

NOTE: For this equation we use only 15-time steps because for short Δt we do not obtain good results. These time steps are listened in table 19.

Box 25

Table 19

Position of each used Δt.

Pos	Δt in sec	Pos	Δt in sec	Pos	Δt in sec
1	2e-05	6	0.0008	11	0.04
2	4e-05	7	0.002	12	0.08
3	8e-05	8	0.004	13	0.2
4	0.0002	9	0.008	14	0.4
5	0.0004	10	0.02	15	0.8

Figure 7 and 8 show the solution by using some data; while figure 7 show the obtained results, figure 8 show the error taking Laplace method like a reference.

ISSN: 2410-3454.
RENIECYT-CONAHCYT: 1702902

Box 26

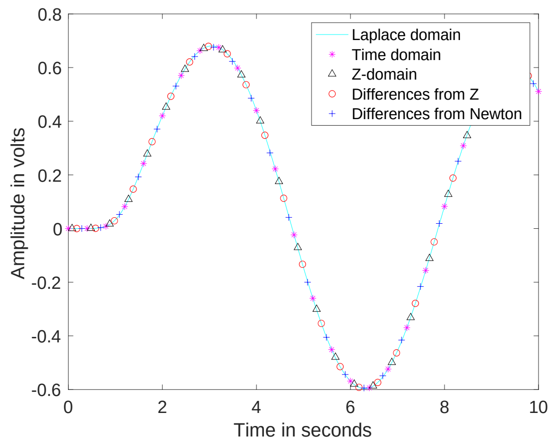

Figure 7

a) Solution by Laplace, z-transform and equation in differences

Box 27

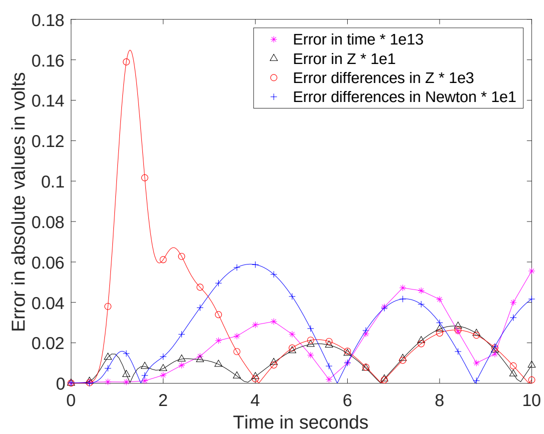

Figure 8

Error taking Laplace like a reference

Table 20 shows the best solution, that means, the time steps for which we obtain the lowest error according with the used error.

Box 28

Table 20

Errors using different values for A, B, C and F

A=-1e4*w^2, B=-2e6*w, C=0 and F=60 Hz.

Kind of error	Time domain	Z-domain	Differences from Z	Differences Newton
MSE_{Error}	6.342e-30	2.0295e-06	2.0983e-09	1.0377e-05
	15	12	10	9
	6.494e-30	2.0813e-05	1.8988e-08	2.5187e-05
	1	11	11	10
$AREA_{Erro}$	2.3834e-16	0.0030792	0.00022538	0.0084913
	1	12	10	10
	2.3836e-16	0.019035	0.00066846	0.0090726
	7	13	11	9
$\%_{Error}$	3.8934e-17	0.00044361	3.3041e-05	0.0012562
	15	12	10	10
	5.0282e-17	0.0026695	9.7801e-05	0.0013342
	3	13	11	9

Conclusions

Figure 2 shows the first cycles of the simulation and the error taking as a reference the analytical solution, which was obtained with the Laplace transform. Likewise, Figure 3 shows the long-term simulation, that is, until both the results obtained with the z transform and those of the difference equation based on this transform are apparently stabilized.

At first glance it can be seen how the results obtained starting from the z-transform have an increasing error, the reason is that a sinusoidal function is used as a source and the roots that must be obtained are, however when doing the analysis, they are. They remained in position 4 and 5 of the vector of roots and have an error of, this error, although very small, increases as the number of samples advances. This error of course is strictly numerical but it cannot be removed because it is part of the entire numerical process, that is, if it is arbitrarily removed, the solution is not improved.

Declarations

Conflict of interest

The authors declare no interest conflict. They have no known competing financial interests or personal relationships that could have appeared to influence the article reported in this article.

Author contribution

Gutiérrez-Robles, José Alberto: Development of the algebra of the methods proposed here.

Galván-Sánchez, Verónica Adriana: Programming the methods presented in the article

Bañuelos-Cabral, Eduardo Salvador: Review, generation and selection of the examples and/or results presented in the article.

De La Cruz-García, Elba Lilia: Review of the content, putting the article into format and translation into English.

Availability of data and materials

All the results that are obtained are in the article and can be accessed freely depending on the journal's policies.

ISSN: 2410-3454.
RENIECYT-CONAHCYT: 1702902

Journal of Engineering Applications December 2024 Vol.11 No.32 1-19
Article

Funding

The cost of publishing this work in the journal is absorbed by the University of Guadalajara.

Acknowledgements

We thank the University of Guadalajara for funding the publication of this work in the journal.

Abbreviations

HOODE	High-Order Ordinary Differential Equations
ITLS	Invariant in Time Linear Systems
MSE	Mean Square Error
ODE	Ordinary Differential Equation

References

Antecedents

Burden, L. R. & Faires, J. D. (2016). Numerical analysis. 10th edition, ISBN: 1305253663, Brooks/Cole 20 Channel Center Street, Boston MA 002210 USA., Publicher: CENGAGE.

Hoffman, J. D. (2001). Numerical methods for engineers and scientists. Marcel Dekker, Inc. New York. ISBN: 0-8247-0443-6. Word Wide Web.

Basics

Hsu, H. P. (1970). Fourier Analysis. Simon & Schuster, Inc. ISBN: 0671189042.

Lathi, B. P. (2002). Linear Systems and Signals. Berkeley Cambridge Press.

Supports

Noda, T. & Ramirez, A., (2007). z-Transform-Based Methods for Electromagnetic Transient Simulations. *Power Delivery, IEEE Trans on*, ISSN 0885-8977, vol.22, no.3, pp.1799-1805.

Wilcox, D. J., (1978). Numerical Laplace Transformation and Inversion. Int. J. Elect. Enging. Educ., Vol. 15, pp. 247-265.

Saadeh, R., Alshawabkeh, A. A., Khalil, R., Abdoon, M. A., Taha, N., & Almutairi, D. K. (2024). The Mohanad Transforms and Their Applications for Solving Systems of Differential Equations. *European Journal of Pure and Applied Mathematics*, *17*(1), 385-409.

Smith G. D. (1986). Numerical Solution of Partial Differential Equations, Finite Difference Methods. Third Edition, Clarendon Press, Oxford. ISBN: 9780198596509.

Differences

Marciniak, K., Saleem, F., & Wiora, J. (2024). Influence of models approximating the fractional-order differential equations on the calculation accuracy. *Communications in Nonlinear Science and Numerical Simulation*, ELSEVIER, Research paper, Vol. *131*, 107807.

Salas, A. H., El-Tantawy, S. A., & Jairo E, C. H. (2024). On the approximate and analytical solutions to the fifth-order Duffing oscillator and its physical applications. *Waves in Random and Complex Media*, *34*(3), 2000-2020.

Strikwerda J. (2004). Finite Difference Schemes and Partial Differential Equations. Second Edition, Wadsworth & Brooks/Cole Advanced Books and Software, Pacific Grove, California.

Williams, P. W. (1972). Numerical computation. Nelson Edition, boards: 0-17-761018-2, paper: 0-17-771018-7, 191 pages.

Discussions

Golmankhaneh, A. K., & Bongiorno, D. (2024). Exact solutions of some fractal differential equations. *Applied Mathematics and Computation*, Volume: *472*, 128633.

Kinkaid D. R. & Hayes L. J. (2014). Iterative Methods for Large Linear Systems. Academic Press Inc. Hancourt Brace Jovanovich. ISBN-10: 148324167X.

Xiang, R., van Schie, S. P., Scotzniovsky, L., Yan, J., Kamensky, D., & Hwang, J. T. (2024). Automating adjoint sensitivity analysis for multidisciplinary models involving partial differential equations. *Structural and Multidisciplinary Optimization*, *67*(8), 1-31.

ISSN: 2410-3454.
RENIECYT-CONAHCYT: 1702902

Journal of Engineering Applications December 2024 Vol.11 No.32 20-25
Article

Inverter technology and the role of the user behavior: Towards a more efficient use of energy

La tecnología inverter y el rol del comportamiento del usuario: Hacia un uso más eficiente de la energía

Vidal-Santo, Adrián* [a], Campos-Domínguez, Armando [b], Vázquez-Guzmán, Aldo G. [c] and Castillo-Toscano, William A. [d]

[a] ROR Universidad Veracruzana • LIF-3563-2024 • 0000-0002-3133-4332 • 38268
[b] ROR Universidad Veracruzana • LIG-3982-2024 • 0009-0006-8393-1493 • 404710
[c] ROR Universidad Veracruzana • ADA-3560-2022 • 0000-0002-6955-7777 • 867120
[d] ROR Universidad Veracruzana • LIF-7601-2024 • 0009-0003-1385-4523 • 83608

CONAHCYT classification:

Area: Engineering
Field: Technological sciences
Discipline: Mechanical technology and engineering
Subdiscipline: Refrigeration equipment

doi https://doi.org/10.35429/JEA.2024.32.11.20.25

History of the article:
Received: September 01, 2024
Accepted: December 26, 2024

Check for updates

* ✉ [avidal@uv.mx]

Abstract

The article analyzes the energy efficiency of air conditioning (AC) systems with inverter technology compared to On/Off systems, highlighting the importance of user behavior in energy consumption. AC is essential for comfort and health, but it also contributes significantly to CO_2 emissions due to high energy consumption. Inverter technology can reduce energy consumption by maintaining a more stable internal temperature and reducing operating costs and emissions in comparison with On/Off systems. However, incorrect use by users, such as turning the AC to maximum capacity and then reducing it, lead to energy inefficiencies. Thus, users play a crucial role in the control to improve energy efficiency. It has been studied that the participation of users in temperature management and the advanced technologies use optimize energy consumption and reduce environmental impact. i.e., the adoption of inverter systems and user education are essential to achieve a more sustainable and efficient use of energy in hot climate areas.

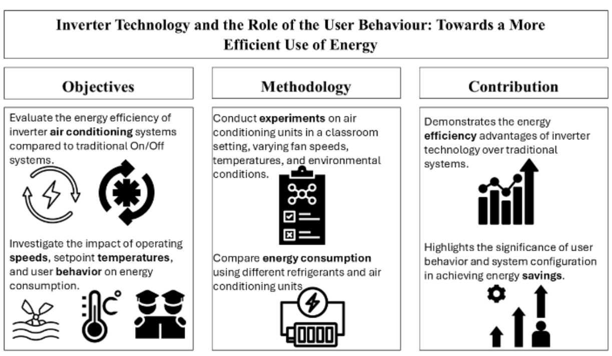

Energy efficiency, Inverter technology analyzes, Energy consumption comparison.

Resumen

Se examina la eficiencia energética de los sistemas de aire acondicionado (AC) con tecnología inverter frente a los sistemas On/Off, subrayando el papel del usuario en el consumo de energía. Aunque el AC es vital para la comodidad y salud, también contribuye a las emisiones de CO_2 debido a su alto consumo energético. La tecnología inverter reduce el consumo de energía al mantener una temperatura interna estable, disminuyendo los costos y las emisiones comparado con los sistemas On/Off. Sin embargo, un mal uso, como ajustar el AC a máxima capacidad y luego reducirlo, provoca ineficiencias energéticas. Por lo tanto, el comportamiento del usuario es crucial para mejorar la eficiencia energética. Se estudió que la participación activa en la gestión de la temperatura y el uso adecuado de tecnologías avanzadas optimizan el consumo energético. La adopción de sistemas inverter y la educación del usuario son esenciales para un uso más sostenible y eficiente en climas cálidos.

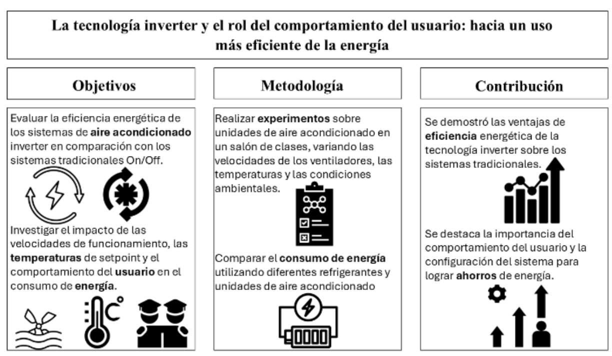

Eficiencia energética, análisis de tecnología inverter, comparativo de consumo energético.

Citation: Vidal-Santo, Adrián, Campos-Domínguez, Armando, Vázquez-Guzmán, Aldo G. and Castillo-Toscano, William A. Inverter technology and the role of the user behavior: Towards a more efficient use of energy. Journal of Engineering Applications. 2024. 11-32: 20-25.

Journal of Engineering Applications December 2024 Vol.11 No.32 20-25
Article

Introduction

Air conditioning in hot areas is mainly used for thermal comfort and public health reasons. In regions where temperatures reach high levels, especially during the summer, air conditioning provides a comfortable and safe environment by reducing the temperature and humidity of the indoor air. This is crucial for preventing heat-related health problems, such as heat stroke and dehydration, which can negatively affect vulnerable populations such as young children, the elderly, and people with chronic illnesses (Ebi et al., 2021).

However, the widespread use of air conditioning carries significant consequences for global climate change. The main impact comes from energy consumption (Hilmiyati-Mas'adah et al., 2023). Fossil fuels make up 80% of current global primary energy demand, and the energy system generates around two-thirds of global CO_2 emissions (Adu et al., 2024).

This additional demand for electricity to power air conditioning systems can directly contribute to greenhouse gas emissions, exacerbating global warming and climate change. Therefore, while air conditioning is crucial for human well-being in hot areas, it is imperative to develop and adopt more efficient and sustainable technologies, such as less energy-intensive refrigeration systems (Foster & Elzinga, 2024).

An alternative is inverter technology, which adjusts the compressor speed according to the thermal demand. This reduces energy consumption by up to 35% compared to traditional systems, maintaining a more stable indoor temperature and reducing operating costs and CO_2 emissions (Siriwardhana & Namal, 2017). Implementing this technology in air conditioning systems is a step towards greater energy efficiency and sustainability (Ebeed et al., 2024).

Although the inverter system in air conditioners is an advanced technology that promises energy efficiency, its incorrect use by users can generate contrary results. Many users turn the air conditioner on to full capacity at first and then reduce it, which can lead to periods of overcooling or overheating, thus increasing unnecessary energy consumption.

This pattern of manual use, where the user sets the air conditioner to its maximum power and then decreases it, creates considerable energy inefficiencies. According to Liu et al. (2021), the lack of use of automatic control in these systems results in higher energy consumption due to human intervention and inconsistent usage patterns. It is crucial to highlight the importance of including occupants in the control system of air conditioners to improve energy efficiency. Research has shown that including users in this process is not only an economical methodology but also effective for detecting occupancy and collecting data on user behavior (Zhou et al. 2024), thus contributing to a more efficient use of energy(Tang et al., 2021).In particular, the energy consumption due to the use of air conditioners in hot humid areas such as the port of Veracruz, Mexico, represents around 80% of the total kWh during the spring, summer, and early season periods in the educational sector (Vidal, 2016).

Methodology

Two power grid analyzers were used to record energy consumption when air conditioning (AC) equipment was operated simultaneously. In the experimentation, the set point of the operating temperatures (Interior Comfort Temperature), the evaporator fan speeds, and of course the time evolution of the ambient temperature corresponding to each monitoring cycle, during more than a year of experimentation, were varied; since the seasonal efficiency of the equipment (Resource Efficiency and Environmental Efficiency, REEE) will depend on the uses and habits of the user and of course on the environmental conditions.

In terms of energy efficiency, R32 refrigerant is typically slightly more efficient than R410A due to its higher thermal conductivity and lower vapor pressure, allowing air conditioning systems to use less energy to achieve the same cooling capacity. It is estimated that this difference can translate into an energy efficiency improvement of around 5% isotropic efficiency compared to R410A, depending on the specific operating conditions of the equipment. The characteristics of each AC equipment that was experimented with are presented in Table 1 (Bobbo et al., 2019; Kim et al., 2023).

ISSN: 2410-3454.
RENIECYT-CONAHCYT: 1702902

Vidal-Santo, Adrián, Campos-Domínguez, Armando, Vázquez-Guzmán, Aldo G. and Castillo-Toscano, William A. Inverter technology and the role of the user behavior: Towards a more efficient use of energy. Journal of Engineering Applications. 2024. 11-32: 20-25
https://doi.org/10.35429/JEA.2024.32.11.20.25

Box 1

Table 1

The characteristics of each air conditioning unit used in the experiment

Characteristics	Inverter Mirago	Inverter Carrier	On/Off Mirago
Capacity (BTU/hr)	12000	12000	12000
Refrigerant	R-32	R-410A	R-410A
Reported REEE (BTUh/We)	16.8	16.8	12.1

Source: (Bobbo et al., 2019; Kim et al., 2023).

The air conditioning (AC) systems were installed in a classroom of 32 m^2 or 90 m^3, in which 32,000 BTU of thermal load is required: so. In the experimentation, the 12,000 BTU systems were complementary to the 24,000 BTU system that exists in the room. In the first stage of testing, the 12,000 BTU equipment was operated alternately and was energized to 220 V. The electrical network analyzer was configured to the voltage operated by the equipment and although many electrical parameters were monitored, this study focuses mainly on energy consumption (kWh). The period of operation, in the first stage, of the AC equipment was, in most cases, from 09 to 14 and from 16 to 19 h, with some variations, and in the second stage only from 09 to 14 h. The room contained an average of 11 people during the experimentation, in the first stage, and an average of 5 people, during the second stage.

During the experiment, temperatures inside and outside the room were recorded using J-type thermocouples. Data acquisition was done using trademark technology and software, and the complete design of the SCADA system is described in detail in another article written by the same authors (Campos-Domínguez et al., 2024). In the second stage of the experimentation, only inverter systems of two different brands were worked on, which were also operated alternately and simultaneously.

Results

Figure 1 shows the comparison of energy consumption as a function of ambient temperature for two devices, both with inverter technology, operating at different setpoint temperatures: 24°C (a), 23°C (b), and 22°C (c), with the fan speed in medium configuration.

In each of these scenarios, a consistent trend of reduction in energy consumption is observed in the Carriero equipment (solid blue line). This decrease in consumption could be due to the technology of each of the manufacturers concerning the compressor, evaporator, and condenser fans since the Carriero is mid-range equipment that is 30% more expensive than the Mirago.

Box 2

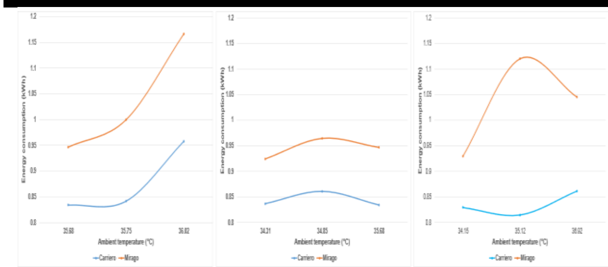

Figure 1

Comparison of energy consumption as a function of the ambient temperature of two inverter units operating at a setpoint temperature of 24°C (a), 23°C (b), and 22°C (c) and intermediate fan speed

Figure 2 explores the power consumption as a function of the setpoint temperature, again using two inverter units operating at average fan speed. The comparison between different setpoints shows a clear trend. For ambient temperatures between 36 and 37 °C, which represents a very hot day with thermal sensations of around 45°C, inverter technology is more appreciated in the AC Carriero at a set point of 24°C and this energy consumption gap is reduced as the setpoint decreases, that is, the colder the equipment is required.

Box 3

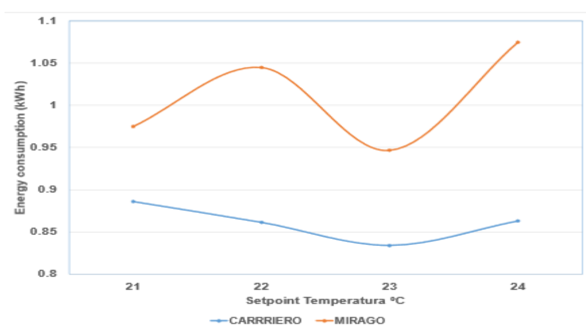

Figure 2

Comparison of energy consumption as a function of setpoint temperature of two inverter units operating at intermediate fan speed

Journal of Engineering Applications December 2024 Vol.11 No.32 20-25
Article

Moreover, Figure 3 presents a comparison of energy consumption as a function of ambient temperature, contrasting equipment with inverter technology (blue line) and a device with On/Off technology (orange line) operating at setpoint temperatures of 22°C (a) and 23°C (b) with medium fan speed. This figure highlights the significant differences in energy performance between the two technologies. Inverter systems show significantly lower energy consumption compared to On/Off systems, particularly at higher temperatures. The blue line, representing the inverter system, shows a flatter and more stable curve, indicating a better ability to maintain energy efficiency regardless of fluctuations in ambient temperature. In contrast, the orange line of the On/Off system shows more inefficient energy consumption due to the need to turn the compressor on and off repeatedly to maintain the desired temperature.

The energy consumption behavior of two inverter air conditioning units, Carriero and Mirago, was evaluated in high and medium-speed configurations within a setpoint temperature range of 21-24°C and an ambient temperature of 36-37°C (Figure 1). The results show significant differences in energy consumption (kWh) between the two operating speeds for each unit, highlighting the importance of an appropriate selection of the operating speed to optimize energy efficiency. Under high-speed conditions, the Carriero unit maintains relatively stable power consumption through the various setpoint temperatures, with a slight increase to 22°C, followed by a gradual decrease towards 24°C. On the other hand, the Mirago unit exhibits greater fluctuation, reaching its peak consumption at 22°C and drastically reducing afterward. This variability in Mirago suggests lower operational efficiency at high speed compared to Carriero.

Consequently, when comparing the high- and medium-speed configurations, it is observed that both units show a reduction in energy consumption when operating at medium speed. The Carriero unit, in particular, stands out for its more consistent and lower consumption profile at medium speed, which highlights its superior efficiency in this configuration. Similarly, although the Mirago unit also reduces its consumption at medium speed, its fluctuation pattern persists, with a peak at 22°C before decreasing.

Our results show the importance of proper use of speed settings in inverter air conditioning systems to maximize energy efficiency. As Liu et al. (2021) mention, the incorrect use of these advanced technologies, such as frequent manual adjustment of maximum power, can lead to significant inefficiencies. In this context, it is crucial to promote the use of automatic control and the participation of occupants in the temperature management process, as shown by the research of Tang et al. (2021), showing that the inclusion of users as a relevant factor in energy studies not only improves energy efficiency but also optimizes occupancy detection and the collection of data on user behavior. This comparative analysis between operating speeds highlights that choosing the right speed can result in considerable energy savings and more efficient use of inverter air conditioning systems, especially in high-temperature environments.

The Carriero unit, with its remarkable performance at medium speed, demonstrates how an optimized operating setup can contribute significantly to energy efficiency as can be reported in other investigation cases (Hrouda et al., 2024; Liu et al., 2021).

Box 4

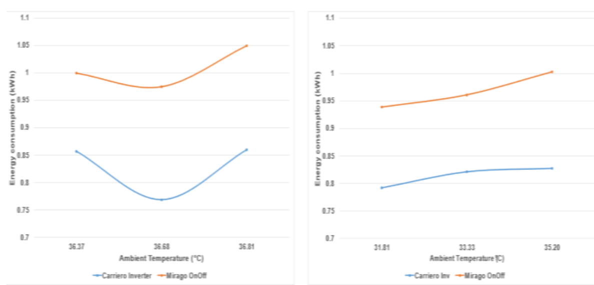

Figure 3

Comparison of energy consumption based on the ambient temperature of two units, the blue line is from the inverter and the orange line is from the On/Off operating at a setpoint temperature of 22°C (a), and 23°C (b) and intermediate fan speed

Conclusions

This study highlights the importance of choosing the right operating speed in air conditioning systems to maximize energy efficiency. It was noted that although the Carriero unit is more expensive, it provides more stable and efficient performance than the Mirago unit, especially at medium speeds.

ISSN: 2410-3454.
RENIECYT-CONAHCYT: 1702902

Vidal-Santo, Adrián, Campos-Domínguez, Armando, Vázquez-Guzmán, Aldo G. and Castillo-Toscano, William A. Inverter technology and the role of the user behavior: Towards a more efficient use of energy. Journal of Engineering Applications. 2024. 11-32: 20-25
https://doi.org/10.35429/JEA.2024.32.11.20.25

Journal of Engineering Applications December 2024 Vol.11 No.32 20-25
Article

This superior performance is partly attributed to the use of R-410a refrigerant in the Carriero unit, which proves to be more effective in reducing energy consumption in high-temperature conditions compared to the R-32 refrigerant employed by the Mirago unit. These results underscore the need to consciously employ advanced technologies to optimize energy efficiency and mitigate environmental impact. In addition, they open the door to future research on the incorporation of emerging technologies such as machine learning and artificial intelligence into air conditioning systems. Such technologies could bring significant improvements in energy efficiency by dynamically adjusting operating speeds in real time, taking into account environmental conditions and usage patterns. By adopting these innovations, a smarter and more sustainable use of air conditioning systems could be achieved, thus contributing to the reduction of overall energy consumption and developing greener solutions.

Conflict of interest

The authors declare no interest conflict. They have no known competing financial interests or personal relationships that could have appeared to influence the article reported in this article.

Author contribution

Vidal-Santo, Adrian: Contributed to the conceptualization, writing-original draft, data curation, methodology, formal analysis, and project administration.

Campos-Domínguez, Armando: Contributed to the methodology, resources and Investigation.

Vázquez-Guzmán, Aldo: Contributed to the formal analysis, writing-original draft, writing-review & editing.

Castillo-Toscano, William A.: Contributed to the conceptualization, methodology, formal analysis, and project administration.

Availability of data and materials

The data used or analyzed during the current study is available from the corresponding author upon reasonable request.

Funding

The research did not receive any financing.

Acknowledgments

The authors extend their appreciation to the Energy Systems Laboratory of the Veracruz University, Veracruz Region, for generously conceding permission to utilize their facilities. Furthermore, gratitude is expressed to the Faculty of Mechanical Engineering and Naval Sciences of the Mechanical Electrical Engineering Educational Program.

Abbreviations

AC	Air conditioner
REEE	Resource Efficiency and Environmental Efficiency
SCADA	Supervisory Control and Data Acquisition

References

Antecedents

Adu, D., Jianguo, D., Asomani, S. N., & Abbey, A. (2024). Energy generation and carbon dioxide emission—The role of renewable energy for green development. In Energy Reports (Vol. 12, pp. 1420–1430). Elsevier Ltd.

Ebi, K. L., Capon, A., Berry, P., Broderick, C., de Dear, R., Havenith, G., Honda, Y., Kovats, R. S., Ma, W., Malik, A., Morris, N. B., Nybo, L., Seneviratne, S. I., Vanos, J., & Jay, O. (2021). Hot weather and heat extremes: health risks. The Lancet, 398(10301), 698–708.

Foster, S., & Elzinga, D. (n.d.). Naciones Unidas. El Papel de Los Combustibles Fósiles En Un Sistema Energético Sostenible. Retrieved August 21, 2024

Hilmiyati-Mas'adah, H., Sudiro, A., Rohman, F., Yuniarinto, A., Hakam, D. F., & Nugraha, H. (2024). Switching from LPG to electricity in Indonesia: a study in the Java Bali grid. Cogent Business & Management, 11(1), 2298221.

ISSN: 2410-3454.
RENIECYT-CONAHCYT: 1702902

Basics

Ebeed, M., Hashem, M., Aly, M., Kamel, S., Jurado, F., Mohamed, E. A., & Abd El Hamid, A. M. (2024). Optimal integrating inverter-based PVs with inherent DSTATCOM functionality for reliability and security improvement at seasonal uncertainty. Solar Energy, 267, 112200.

Liu, H., Sun, H., Mo, H., & Liu, J. (2021). Analysis and modeling of air conditioner usage behavior in residential buildings using monitoring data during hot and humid season. *Energy and Buildings*, *250*.

Siriwardhana, M., & Namal, D. D. A. (2017). Comparison of Energy Consumption between a Standard Air Conditioner and an Inverter-type Air Conditioner Operating in an Office Building. *SLEMA Journal*, *20*(1–2), 1.

Support

Bobbo, S., Fedele, L., Curcio, M., Bet, A., De Carli, M., Emmi, G., Poletto, F., Tarabotti, A., Mendrinos, D., Mezzasalma, G., & Bernardi, A. (2019). Energetic and Exergetic Analysis of Low Global Warming Potential Refrigerants as Substitutes for R410A in Ground Source Heat Pumps. *Energies*, *12*(18), 3538.

Kim, M. K., Lee, H., & Jeong, J. H. (2023). Evaluation of correlations for mass flow rate of refrigerant through electronic expansion valve in air—water heat pump system using R32. *International Journal of Refrigeration*, *151*, 267–277.

Tang, R., Wang, S., & Sun, S. (2021). Impacts of technology-guided occupant behavior on air-conditioning system control and building energy use. *Building Simulation*, *14*(1), 209–217.

Zhou, T., Chen, H., Zhang, N., Han, Y., Zhou, S., Li, Z., & Zhou, M. (2024). An analogue on/off state-switching control method suitable for inverter-based air conditioner load cluster participating in demand response. Applied Energy, 363, 123096.

Discussions

Campos-Domínguez, A., López-Huerta, F., Castillo-Toscano, W. A., Vázquez-Guzmán, A. G., & Vidal-Santo, A. (2024). Desarrollo de un sistema SCADA con adquisición de temperaturas para comparación de eficiencia térmica de aires acondicionados. *Ingeniantes*, *2*, 36–42.

Hrouda, J. O. S. E. F., Čerňan, M. A. R. T. I. N., & Procházka, K. A. R. E. L. (2024). A New Method of Smart Control of Single-Phase Photovoltaic Inverters at Low Voltage for Voltage Control and Reactive Power Management. *IEEE Access*.

Vidal, A. (2016). Estrategias para mejorar la eficiencia energética y la sustentabilidad en los espacios bibliotecarios. In *Sustentabilidad en el entorno bibliotecario y de la información* (pp. 51–82).

ISSN: 2410-3454.
RENIECYT-CONAHCYT: 1702902

Journal of Engineering Applications December 2024 Vol.11 No.32 26-35
Article

Methodological proposal for the topographic use of UAV compared to the use of traditional methods

Propuesta metodológica para el uso topográfico de UAV respecto al uso de métodos tradicionales

Rodríguez-González, José Miguel*[a], Gómez-Arizmendi, Gabriela [b], Velázquez-García, Jennyfer [c] and Carranza-Reyes, Roberto [d]

a ROR Tecnológico Nacional de México/TES Valle de Bravo • LIG-4761-2024 • 0000-0002-3837-7490 • 1349637
b ROR Tecnológico Nacional de México/TES Valle de Bravo • LIG-4897-2024 • 0009-0004-5805-149X • 1350520
c ROR Tecnológico Nacional de México/TES Valle de Bravo • LIK-4505-2024 • 0009-0009-5325-0576 • 2062853
d ROR Tecnológico Nacional de México/TES Valle de Bravo • LIO-8300-2024 • 0009-0001-4680-224X • 2063155

CONAHCYT classification:

Area: Physics-Mathematics and Earth Sciences
Field: Earth and space sciences
Discipline: Geography
Subdiscipline: Topographic geography

https://doi.org/10.35429/JEA.2024.32.11.26.35

History of the article:
Received: September 01, 2024
Accepted: December 26, 2024

* ✉ [jose.rg@vbravo.tecnm.mx]

Abstract

A methodology for topographic surveys using a UAV is presented, conducted at the Tecnológico de Estudios Superiores de Valle de Bravo (TESVB) with a DJI Phantom 4 Pro RTK drone, DJI GNSS DRTK2 mobile station, and Agisoft Metashape software. The objective is to propose an effective and precise methodology compared to traditional methods. The simplified approach allows for accurate position and processing information, generating digital terrain models. The results offer an efficient alternative, reducing time by 46.66% with a relative error of 0.64% in linear measurements and 0.42% in area measurements. Additionally, the UAV's ability to access various areas and capture real-time data is a significant advantage. This study demonstrates the potential of UAVs in topographic applications, although further analysis in different environments is necessary to fully validate their applicability and accuracy.

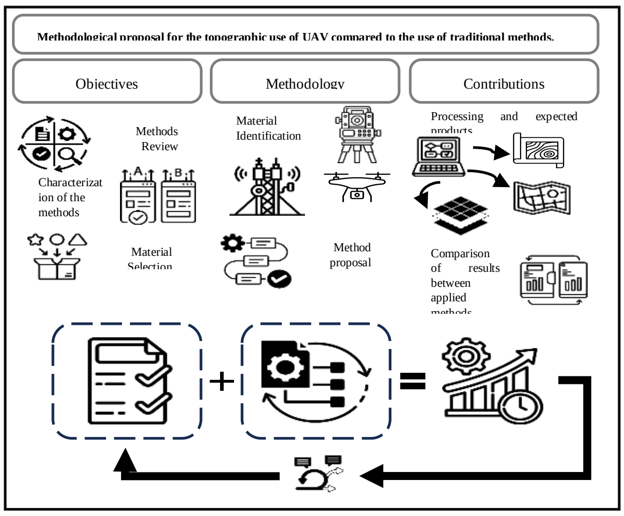

Methodological, Topographic, Unmanned

Resumen

Se presenta una metodología para levantamientos topográficos con un UAV, realizada en el Tecnológico de Estudios Superiores de Valle de Bravo (TESVB), utilizando un dron DJI Phantom 4 Pro RTK, estación móvil DJI GNSS DRTK2 y el software Agisoft Metashape. El objetivo es proponer una metodología eficaz y precisa comparada con métodos tradicionales. El enfoque simplificado permite obtener información precisa de posición y procesamiento, generando modelos digitales del terreno. Los resultados ofrecen una alternativa eficiente, reduciendo el tiempo en un 46.66% y con un error relativo del 0.64% en medidas lineales y 0.42% en el área. Además, la capacidad del UAV para acceder a diversas áreas y capturar datos en tiempo real es una ventaja significativa. Este estudio demuestra el potencial de los UAV en aplicaciones topográficas, aunque es necesario un análisis adicional en distintos entornos para validar completamente su aplicabilidad y precisión.

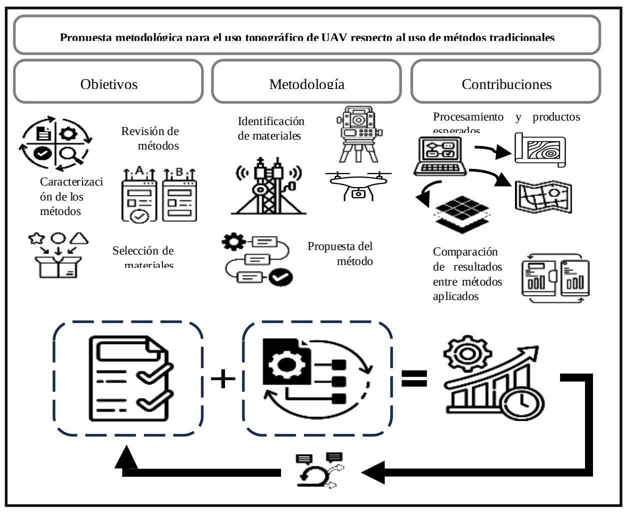

Metodológico, Topografía, No tripulado

Citation: Rodríguez-González, José Miguel, Gómez-Arizmendi, Gabriela, Velázquez-García, Jennyfer and Carranza-Reyes, Roberto. Methodological proposal for the topographic use of UAV compared to the use of traditional methods. Journal of Engineering Applications. 2024. 11-32: 26-35.

Journal of Engineering Applications December 2024 Vol.11 No.32 26-35
Article

Introduction

Surveying is an essential component of civil engineering. Its theory is mainly based on plane geometry, space geometry, trigonometry and mathematics in general.

Several authors define topography as the science through which positions of points located on the earth's surface, above and below it, can be established; therefore, measurements such as linear and angular distances and elevations are carried out (Mark & Smith, 2004; Rincón Villalba, et al., 2017).

Although the conceptualisation of topography has not changed over the years, the techniques, instruments and methods of application have been modified and increased, all generated by technological progress, from the use of the tape measure, theodolites and the total station.

Technological advances have revolutionised the way in which surveying is carried out, allowing accurate and detailed data to be obtained more efficiently. Particularly the use of Unmanned Aerial Vehicles (UAVs) has gained popularity for their ability to collect data in difficult to access areas and their versatility in generating three-dimensional terrain models (Remondino, et al., 2011; Westoby, et al., 2012).

Ground survey methods have undergone a complete transformation, keeping the accuracy of the product comparable to that of field surveys (Bangen, et al., 2014). High accuracy is not feasible even with digital aerial surveys due to flight height limitations. Technically, UAVs can fly virtually anywhere. Due to their high flexibility, the location of the platform and its viewing angle can be changed in a short time (Lyu, et al., 2023). Even with low-cost commercially available UAVs, flying at low altitudes is no longer a problem for the photogrammetry user community (Kršák, et al., 2016).

Thus, it is possible to obtain images with very high Ground Sampling Distance (GSD), close to 1 cm, which allows users to achieve remarkable positional accuracy without much effort.

Although low-cost drones are used in topographic surveys, there is still debate as to which platform, hardware and software are best suited to achieve the accuracy required for high quality surveys. With a sufficient number of accurate Ground Control Points (GCPs) and an on-board Real Time Kinematic (RTK) Positioning system with an accurate Inertial Measurement Unit (IMU), the desired accuracy can be easily achieved (Famiglietti, et al., 2024; Martinez-Fernandez, et al., 2024).

GCPs should be carefully selected, well distributed and visible in multiple images. Moreover, they must be easily identifiable in the images obtained.

On the other hand, with Unmanned Aerial Systems (UAS), the recurrent data acquisition that many studies require can be performed at any time. This is, of course, not possible with super-high-resolution satellite imagery that has a fixed temporal resolution. This is another factor contributing to the popularity of UAS (Awasthi, et al., 2020).

Some of the best classified methodological developments contain structures that do not depend on the software used but on the techniques employed, i.e. to scan a large area of land, such as a topographic map, a similar methodology is applied as developed with traditional methods, except that the photos would form a 'blanket' over the extent of a balloon site. Such forms of photogrammetry are usually carried out using UAVs. A topographic survey and mapping using photogrammetry has been gaining popularity due to its competitiveness; fast result, low cost and high accessibility (Lim, et al., 2021).

The techniques to be used and methods developed depend on the type of applicability, which is why the precise definition of a methodology is complex, as it depends on the context, equipment and even the experience of the practitioners (Rus, et al., 2024).

Background

With the variety of products on the market today, it is difficult to define a specific methodology, as there are different variables that determine it, the literature has interesting proposals;

ISSN: 2410-3454.
RENIECYT-CONAHCYT: 1702902

Rodríguez-González, José Miguel, Gómez-Arizmendi, Gabriela, Velázquez-García, Jennyfer and Carranza-Reyes, Roberto. Methodological proposal for the topographic use of UAV compared to the use of traditional methods. Journal of Engineering Applications. 2024. 11-32: 26-35
https://doi.org/10.35429/JEA.2024.32.11.26.35

Wu, et al. (2020) reported a process that includes the steps; 1) flight range determination, 2) obtaining control points, 3) aerial point installation, 4) flight plan simulation, 5) flight mission, 6) photo classification, 7) photo scanning and 8) layer fitting. This is without reporting the type of drone and software used.

Karakiş, et al. (2020) writes an ambiguous but effective method, which consists of; 1) identification of the study area, 2) flight planning, 3) data processing and 4) data correction. He uses an octocopter with a Canon EOS 450D camera and does not report the software used in the processing.

Devoto, et al., (2020) carried out a process in which they describe 3 general phases that include stages; I) Data collection, II) Post processing (Control points, 3D Models, DEMs and Orthomosaics) and III) Digitisation and data storage (map and image characterisation), using a DJI Mavic drone and with the use of two softwares Agisoft Metashape and QGIS.

Cortes Ospina (2021) proposes 4 phases; flight planning, ground support, photographic registration, image processing and calculations, using a 6-propeller multi-helicopter with a Canon EOS M camera and Agisoft Photoscan processing software.

Hao et al., (2023) outlines the following steps; 1) site survey, 2) UAV route planning, 3) flight height, speed and overlap rate adjustment, 4) ground control point (GPS) layout, 5) aerial photography, image collection, 6) image processing, 3D point cloud modelling, 7) discontinuity extraction and 8) accuracy verification. Using a DJI Matrice 300 RTK drone and GeoSMA-3D processing software.

Astor, et al. (2023), by means of an analysis to know the conditions of the working pavement by means of; 1) problem identification (drone flight on the road), 2) definition of potential solutions (3D model by means of image capture), 3) behaviour study (Study of the images) and 4) analysis and evaluation (Statistical evaluation and comparison with conventional methods). A DJI Phantom 4 Pro drone, geodetic GPS and Agisoft Methashape software were used in the study.

Wang, et al. (2023), in their reported work for bridge risk analysis opts for the phases of; 1) flight plan, 2a) 3D reconstruction, 3a) visualisation of geometric variables, 4a) capacity model, 4a.a) demand model, and 2b) location, 3b) safety verification and 4b) seismic hazards. Using a DJI Mavic 2 Pro drone and Agisoft Metashape Software

Dmytro Stelmakh, et al. (2024), the methodology he writes deals with the reconstruction of a structure takes a method based on; a) flight plan, b) taking photographs, c) analysis of photographs and detection of defects, d) construction of the 3D model and e) recommendation of the defects found. Using a DJI AIR 2S drone and 3DF Zephyr software.

On the other hand, Siafali & Tsiorias (2024), in their study using UAVs present an approach for surface deformation estimation in road and forest trail networks, using a fixed-wing SenseFly eBee drone, mounted with a 3D S.O.D.A. camera and using PIX4Dmapper software, where they propose; 1) area survey, 2) flight planning, 3) data collection, 4) data processing and model generation.

In a comparative study of sensors, recently in Italy Ciccone et al. (2024), carried out a survey study of an archaeological site, where they compared the use of multispectral sensors mounted on two drones; a DJI Phantom Multespectral drone and a DJI Mavic Enterprise Advanced drone, using the PIX4D Field software, were able to obtain images in different seasons of the year and thus have a survey study with a substantial amount of data.

Materials and Method

In the quest to propose a method that is based on the context of conducting the survey, this work represents a technological advance that enters into the revolution of the way topographic surveys are conducted, marking a significant difference with the methods of the 'past'. Previously, topographic surveys were first carried out with tape-measure measurements. Then, with technological advances, the theodolite appeared, and finally the total station was introduced. In this field, the DJI Phantom 4 Pro RTK drone (Figure 1) has emerged as a tool in geospatial data capture, thanks to its centimetre accuracy and its ability to integrate Global Positioning Systems (GPS) and satellite navigation.

ISSN: 2410-3454.
RENIECYT-CONAHCYT: 1702902

Journal of Engineering Applications December 2024 Vol.11 No.32 26-35
Article

Box 1

Figure 1
Dron DJI Phantom 4 RTK with remote control

The DJI DRTK 2 GNSS mobile antenna (Figure 2) was also used, which provides real-time differential data, allowing centimetre-accurate positioning to be achieved. The integrated high gain antenna ensures better reception of signals from multiple satellites, even in situations where the signal is obstructed.

Box 2

Figure 2
Mobile antenna GNSS DJI DRTK 2

On the other hand, we can combine these tools with the features of Agisoft Metashape image processing software, which has proven to be an effective solution for the generation of detailed and accurate topographic models from aerial images.

The purpose of the study is to present a complete methodological proposal for conducting topographic surveys using the DJI Phantom 4 Pro RTK drone, the DJI DRTK 2 GNSS mobile antenna and the Agisoft Metashape software. It should be clarified that the decision was taken to compare the measurements made with a Sokkia iM-50 total station because of the lack of the original plans and otherwise because there are no.

Box 3

Figure 3
Sokkia iM-50 Series Total Station

The DJI Phantom 4 RTK is a drone specifically designed for professional applications in surveying and mapping, precision agriculture, disaster management and environmental research. It features RTK integration that provides centimetre accuracy, making it ideal for work that requires high accuracy in geospatial data collection. (Taddia, Stecchi, 2019).

Box 4

Table 1
DJI Phantom 4 RTK Drone Technical Specification

Technical characteristics	Specification
RTK positioning system	This system allows a horizontal accuracy of 1 cm + 1 ppm (parts per million) and a vertical accuracy of 1.5 cm + 1 ppm, which is significantly higher than conventional GPS systems.
Camera and sensor	1-inch, 20-megapixel CMOS sensor, providing high-resolution (FHD) images. The mechanical shutter eliminates rolling shutter distortion, ensuring clear and accurate images are captured, even when the drone is in motion.
Mapping accuracy	It can generate 3D maps and orthomosaics with aerial survey accuracy,
Flight time	offers a maximum flight time of approximately 30 minutes.
Compatibility with base stations	Compatible with DJI's D-RTK 2 mobile station, which provides real-time differential data for even greater accuracy. In addition, it can be used with RTK NTRIP (Network Transport of RTCM - Internet Protocol) networks to extend its versatility in different environments.

ISSN: 2410-3454.
RENIECYT-CONAHCYT: 1702902

Rodríguez-González, José Miguel, Gómez-Arizmendi, Gabriela, Velázquez-García, Jennyfer and Carranza-Reyes, Roberto. Methodological proposal for the topographic use of UAV compared to the use of traditional methods. Journal of Engineering Applications. 2024. 11-32: 26-35
https://doi.org/10.35429/JEA.2024.32.11.26.35

The DJI DRTK 2 mobile GNSS antenna is a high-precision base station designed to provide real-time differential data to drones and other navigation equipment. This antenna is compatible with a wide range of DJI drones, including the Phantom 4 RTK, Matrice 300 RTK, and other models, allowing them to improve the accuracy of their positioning systems (Taddia, González-García, 2020).

Box 5

Table 2

DJI DRTK 2 GNSS Mobile Antenna Technical Specification

Technical characteristics	**Specification**
Positioning accuracy	Horizontal: 1 cm + 1 ppm Vertical: 2 cm + 1 ppm
Constellations GNSS	GPS: L1, L2 GLONASS: F1, F2 BeiDou: B1, B2 Galileo: E1, E5a
Update frequency	1 Hz, 2 Hz, 5 Hz, 10 Hz, 20 Hz
Communication interface	UART Ethernet OcuSync Wifi 4G
Environmental resilience	Degree of protection IP57 (dust and water) Operating temperature:-20°C-55°C
Compatibility	Drones DJI: DJI Phantom 4 PRO RTK, Matrice 300 RTK Con redes NTRIP (Network Transport of RTCM – internet protocol).

The professional Agisoft Metashape software works for photogrammetric processing of digital images and the generation of 3D geospatial data. It is designed to convert 2D images into accurate three-dimensional models, enabling advanced applications in various fields.

The selected terrain is the esplanade of the Tecnológico de Estudios Superiores de Valle de Bravo, located in the municipality of Valle de Bravo, State of Mexico, Mexico, (Figure 4) coordinates (19°14'18 'N 100°07'53 'W). The terrain definition is shown in Figures 4 and 5, taken using Google Earth.

Box 6

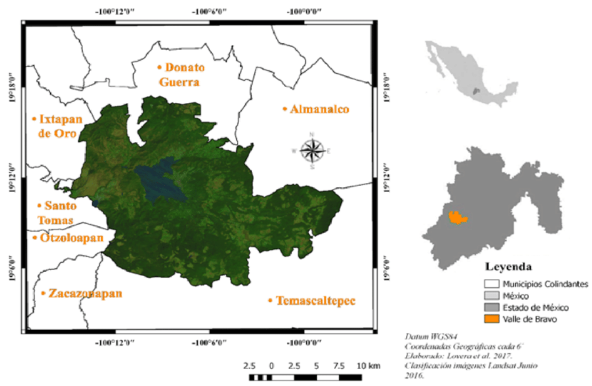

Figure 4

Location of the study site, location of the municipality in the State of Mexico

Box 7

Figure 5

Location of the study site; Tecnológico de Estudios Superiores de Valle de Bravo

Box 8

Figure 6

Location of the study site; exact location within the TESVB

After locating the terrain, a topographic survey was carried out by means of the conventional method using the reported total station, as shown in Figure 7.

Box 9

Figure 7
Carrying out the topographic survey with the total station

Based on the formulation, context and team, the methodology described in Figure 8 is proposed, where we observe the following phases:

Box 10

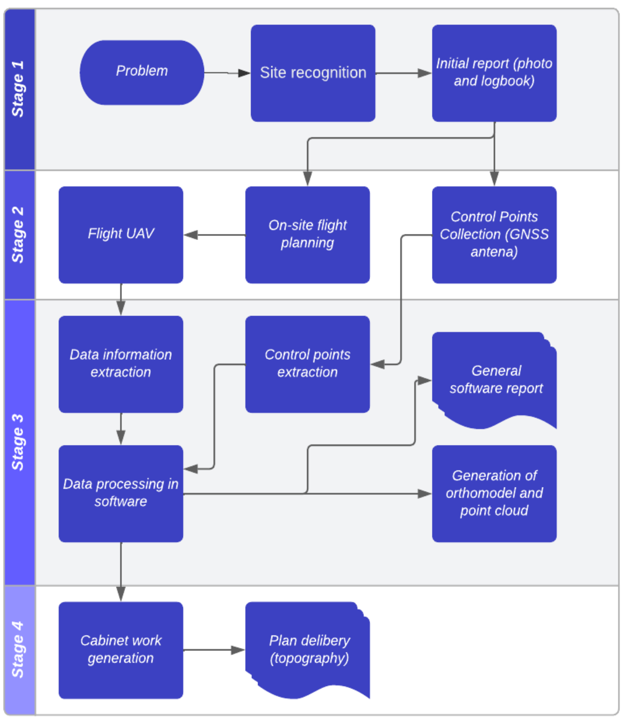

Figure 8
Proposed methodology for surveying with the use of UAV technology

Stage 1

Problem. The justification for the study is defined and the initial measurement parameters are established.

Site reconnaissance. A detailed analysis of the site is carried out, considering the general characteristics of the terrain that will determine the process to be followed.

Initial report. A photographic report of the site is prepared, documenting the characteristics observed.

Stage 2

Taking of control points (GNSS). This process is crucial for the processing and reference of the project.

On-site flight planning: Based on the terrain characteristics, the UAV flight is planned to optimise data collection.

UAV flight: The flight is carried out following the established planning, monitoring any possible inconvenience.

Stage 3

Extraction of control points: The necessary information is collected using the GNSS antenna and the UAV.

Data extraction: The data collected by the UAV is extracted for further processing.

Data processing in software: With the control points and flight data, the data is processed in specialised software.

General software report: A detailed processing report is generated according to the specific characteristics of the project.

Orthomodel and point cloud generation: From the report, the ortho-model and point cloud are extracted to produce the topographic plan.

Stage 4

Generation of the cabinet work: Stakeout work is carried out to generate the final deliverable.

Delivery of plans (topography): Finally, the topographic plans are delivered, ready to be used according to the user's requirements.

Following the aforementioned stages, the terrain survey was carried out using the described materials. The terrain survey is shown in Figure 6, followed by the survey of control points (Figure 9) and flight planning, as shown in Figure 10. A 3D flight was chosen to detect possible irregularities in the terrain, leaving the default settings in the system for this study.

ISSN: 2410-3454.
RENIECYT-CONAHCYT: 1702902

Rodríguez-González, José Miguel, Gómez-Arizmendi, Gabriela, Velázquez-García, Jennyfer and Carranza-Reyes, Roberto. Methodological proposal for the topographic use of UAV compared to the use of traditional methods. Journal of Engineering Applications. 2024. 11-32: 26-35
https://doi.org/10.35429/JEA.2024.32.11.26.35

Journal of Engineering Applications December 2024 Vol.11 No.32 26-35
Article

Box 11

Figure 9

Taking of control points with GNSS mobile stations

Box 12

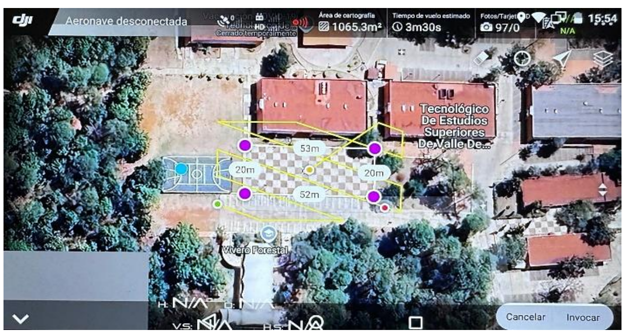

Figure 10

Flight planning, as seen from the UAV control

Subsequently, after the extraction of control points and data, they were processed in specialised software to obtain final products such as the orthomodel and the point cloud. With this information, cabinet work was carried out to generate the polygon plan with the extracted topography. Results and discussion The plan made by the conventional method (Figure 11) allowed the extraction of time data (Table 4) and the reference of the plan. In addition, 3 people worked on it.

Box 13

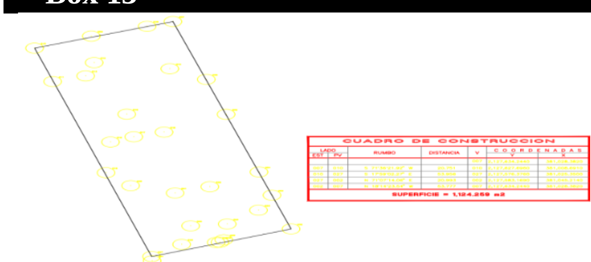

Figure 11

Terrain polygon made with the survey using the total station

Box 14

Table 3

Working time data for each activity in the survey using the total station

Activity	Working time
Survey	90 min.
Processing	20 min.
Cabinet work	40 min.
Total time	150 min.

On the other hand, for the UAV survey, the ortho-model, the point cloud, the polygon generated from the data collection (Figures 12, 13 and 14), together with the working times (Table 4), are presented.

Box 15

Figure 12

Orthomodel enhanced in Agisoft Metashape software

Box 16

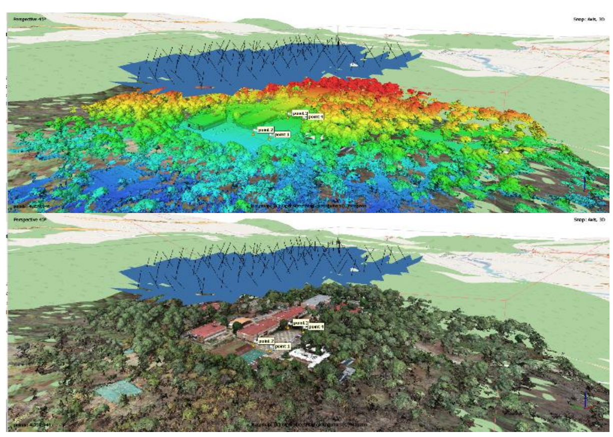

Figure 13

Dense point cloud, showing terrain elevation and photogrammetric elevation

ISSN: 2410-3454.
RENIECYT-CONAHCYT: 1702902

Box 17

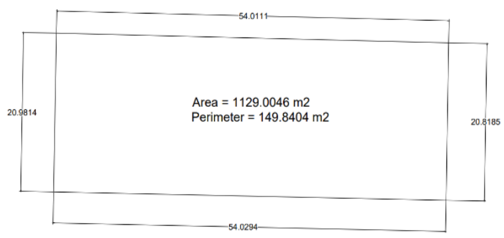

Figure 14
Polygon generated from UAV survey

Box 18
Table 4
Data on the working time of each activity in the UAV survey.

Activity	Tiempo de trabajo
Survey	10 min.
Processing	40 min.
Cabinet work	20 min.
Total time	70 min.

According to Tables 3 and 4, a time reduction of 46.66% is observed compared to the use of the total station. In terms of accuracy, the average relative percentage error of the length of each side of the polygon is 0.64% and the relative percentage error of the area taken is 0.42%, which indicates that the process is relatively efficient, as we have a relative percentage error of less than 1%.

The final products are suitable for end-user use, meeting the requirements of accuracy and usability.

The process is concrete and follows clear steps; however, further testing on more rugged terrain is suggested to assess the capability of the methodology under various conditions.

Conclusions

The proposed methodology is effective for surveying in terrain similar to the one studied, where the topography is not very rugged. However, there is a need to improve the capture of control points in a more efficient way, since, in larger areas or terrain with greater relief, the process may vary due to the processing capacities required.

On the other hand, the time needed to obtain the ortho-model is significantly reduced, which facilitates the creation of a virtual model applicable in several areas beyond topography.
Finally, it is worth mentioning that the methodology fulfils the objective of providing a tool applicable to topographic surveys, although it poses the challenge of improving and testing it in different contexts.

Declarations

Conflict of interest

The authors declare no conflict of interest. They have no known competing financial interests or personal relationships that could have appeared to influence the article reported in this article.

Author contribution

Rodríguez-González, José Miguel: Contributed with the original idea, planning of activities and formulation of the proposed methodology.

Gómez-Arizmendi, Gabriela: Worked with the time management of activities, topographic surveys, flight plans and in the analysis of results and calculation of errors.

Velázquez-García Jennyfer: Undergraduate student who contributed to the characterization of equipment, flight planning and execution, as well as data classification with the drone.

Carranza-Reyes, Roberto: Undergraduate student, who worked on the topographic survey with a total station and drone, generating the technical data for the project.

Availability of data and materials

The data generated are in the custody of the Tecnológico Nacional de México9/TES Valle de Bravo, where they can be made available on request to the corresponding author's email address.

Funding

No external funding was received for the research, it was carried out with resources and funds from the Institute itself.

Journal of Engineering Applications December 2024 Vol.11 No.32 26-35
Article

Acknowledgements

The authors are grateful to the Tecnológico de Estudios Superiores de Valle de Bravo for their support during the development of this work.

Abbreviations

DEMs	Digital Elevation Model
GCP	Ground Control Point
GNSS	Global Navigation Satellite Systems
GPS	Global Positioning System
GSD	Ground Sampling Distance
IMU	Inertial Motion Unit
RTK	Real Time Kinematics
TESVB	Tecnológico de Estudios Superiores de Valle de Bravo
UAS	Unmanned Aerial Systems
UAV	Unmanned Aerial Vehicle

References

Basics

Clair, A. S. (3 de agosto de 2021). *Civil Engineers use math to design, build and maintain transportation structures.* https://azdot.gov/adot-blog/civil-engineers-use-math-design-build-and-maintain-transportation-structures

Mark, D. M., & Smith, B. (2004). A science of topography: Bridging the qualitative-quantitative divide. En M. Bishop, & J. F. Shroder, *Geographic Information Science and Mountain Geomorphology* (75-100).

Rincón Villalba, M. A., Vargas Vargas, W. E., & González Vergara, C. J. (2017). *Topografía: conceptos y aplicaciones.* Bogotá: ECOE Ediciones.

Dargie Chekole, S. (2014). *Surveying with GPS, total station and terresterial laser scaner: a comparative study.* Stockholm, Sweden: KTH.

Remondino, F., Barazzetti, L., Nex, F., Scaioni, M., & Sarazzi, D. (2011). UAV PHOTOGRAMMETRY FOR MAPPING AND 3D MODELING – CURRENT STATUS AND FUTURE PERSPECTIVES –. *Int. Arch. Photogramm. Remote Sens. Spatial Inf. Sci., XXXVIII-1/C22* (págs. 25-31). Zurich, Switzerland: ISPRS.

Westoby, M., Brasington, J., Glasser, N., Hambrey, M., & Reynolds, J. (2012). Structure-from-Motion' photogrammetry: A low-cost, effective tool for geoscience applications. *Geomorphology, 179*(15), 300-314.

Bangen, S. G., Wheaton, J. M., Bouwes, N., Bouwes, B., & Jordan, C. (2014). A methodological intercomparison of topographic survey techniques for characterizing wadeable streams and rivers. *Geomorphology, 206*, 343-361.

Lyu, M., Zhao, Y., Huang, C., & Huang, H. (2023). Unmanned Aerial Vehicles for Search and Rescue: A Survey. *Remote Sensing, 15*(13), 3266.

Kršák, B., Blišťan, P., Pauliková, A., Puškárová, P., Kovanič, Ľ., Palková, J., & Zelizňaková, V. (2016). Use of low-cost UAV photogrammetry to analyze the accuracy of a digital elevation model in a case study. *Measurement*, *91*, 276-287.

Famiglietti, N. A., Miele, P., Memmolo, A., Falco, L., Castagnozzi, A., Moschillo, R., …, Vicari, A. (2024). New Concept of Smart UAS-GCP: A Tool for Precise Positioning in Remote-Sensing Applications. *drones*, *8*(123), 1-16.

Martínez-Fernández, A., Serrano, E., Pisabarro, A., Sánchez-Fernández, M., De San José, J. J., Gómez-Lende, M., Rangel-De Lázaro. Gizéh & Benito-Calvo, A. (2024). The Influence of Image Properties on High-Detail SfM Photogrammetric Surveys of Complex Geometric Landforms: The Application of a Consumer-Grade UAV Camera in a Rock Glacier Survey. *remote sensing, 14*(3528), 1-28.

Awasthi, B., Karki, S., Regmi, P., Dhami, D. S., Thapa, S., & Shankar Panday, U. (2020). Analyzing the Effect of Distribution Pattern and Number of GCPs on Overall Accuracy of UAV Photogrammetric Results. *Proceedings of UASG 2019. Lecture Notes in Civil Engineering. 51*, págs. 339-354. Roorkee, India : Springer, Cham.

Lim, C. H., Zhang, L., & Amaludin, A. E. (2021). Topographic Survey and Modelling using Photogrammetry: A Comparison against Electronic Distance Measurement (EDM) Method. *ASM*, 1-9.

ISSN: 2410-3454.
RENIECYT-CONAHCYT: 1702902

Journal of Engineering Applications December 2024 Vol.11 No.32 26-35
Article

Rus, I., Şerban, G., Breţcan, P., Dunea, D., & Sabău, D. (2024). Identification of Vegetation Surfaces and Volumes by Height Levels in Reservoir Deltas Using UAS Techniques—Case Study at Gilău Reservoir, Transylvania, Romania. *Sustainability, 16*, 648.

Dostal, C., & Yamafune, K. (2020). Photogrammetric texture mapping: A method for increasing the Fidelity of 3D models of cultural heritage materials. *Journal of Archaeological Science: Reports, 18*, 430-436.

Taddia, Y., González-García, L., Zambello, E., & Pellegrinelli, A. (2020). Quality Assessment of Photogrammetric Models for Façade and Building Reconstruction Using DJI Phantom 4 RTK. *Remote Sensing, 12*(19), 3144.

Antecedents

Wu, C.-H., Hsiao, M.-S., & Chang, C.-M. (2020). Utilizing UAV for 3D Map for Urban Land Use in Tainan City, Taiwan. *2nd Eurasia Conference on Biomedical Engineering, Healthcare and Sustainability (ECBIOS)* (págs. 5-7). Tainan, Taiwan,: IEEE.

Karakis, S., Sefercik, U. G., Bilir, T., & Atalay, C. (2020). Precise monitoring of temporal topographic change detection via unmanned. *Bulletin of the Mineral Research and Exploration*, 151-156.

Cortés Ospina, E. J. (2021). Levantamientos topográficos mediante el uso de drones. *INGENIERÍA: Ciencia, Tecnología e Innovación, 8*(2), 111-124.
Hao, J., Zhang, X., Wang, C., Wang, H., & Wang, H. (2023). Application of UAV Digital Photogrammetry in Geological Investigation and Stability Evaluation of High-Steep Mine Rock Slope. *drones, 7*(3), 198.

Supports.

Devoto, S., Macovaz, V., Mantovani, M., Soldati, M., & Furlani, S. (2020). Advantages of Using UAV Digital Photogrammetry in the Study of Slow-Moving Coastal Landslides. *remote sensing, 12*(21), 3566.

Astor, Y., Nebesima, Y., Utami, R., Rouly Sihimbing, A. V., Adli, M., & Rizki Firdaus, M. (2023). Unmanned aerial vehicle implementation for pavement condition survey. *Transportation Engineering, 12*, 100168.

Wang, X., Demartino, C., Narazaki, Y., Monti, G., & Spencer Jr., B. F. (2023). Rapid seismic risk assessment of bridges using UAV aerial photogrammetry. *Engineering Structures, 279*(15), 115589.

Differences

Siafali, E., & Tsioras, P. (2024). An Innovative Approach to Surface Deformation Estimation in Forest Road and Trail Networks Using Unmanned Aerial Vehicle Real-Time Kinematic-Derived Data for Monitoring and Maintenance. *Forests, 15*, 212.

Ciccone, G. (2024). Investigating archaeological remains at Stracciacappe, Rome: comparing traditional sources with UAV-based multispectral, thermal and microtopographic analysis. *Drone Systems and Applications, 12*, 1-16.

Discussions

Dmytro Stelmakh, L. L., Vitalii Diadin, V. S., & Inna Shkurat, O. S. (2024). Damage detection and analysis using unmanned aerial vehicles (UAVs) and photogrammetry method. *VII International Conference "In-service Damage of Materials: Diagnostics and Prediction" (DMDP 2023). 59*, págs. 43-49. Ternopil, Ukraine: Integrity, Procedia Structural.

Taddia, Y., Stecchi, F., & Pellegrinelli, A. (2019). Using Dji Phantom 4 Rtk Drone For Topographic Mapping Of Coastal Areas. *Int. Arch. Photogramm. Remote Sens. Spatial Inf. Sci., XLII-2/W13*, 625-630.

ISSN: 2410-3454.
RENIECYT-CONAHCYT: 1702902

Journal of Engineering Applications December 2024 Vol.11 No.32 36-42

Article

Study of the relationship between uniaxial compressive strength and the point load index test in rocks from the bank in Seybaplaya Campeche Mexico

Estudio de la relación entre la resistencia a la compresión uniaxial y el ensayo de índice de carga puntual en rocas del banco de Seybaplaya Campeche México

Naal-Pech, José Wilber*[a], Palemón-Arcos, Leonardo [b], El-Hamzaoui, Youness[c] and Gutiérrez-Can, Yuriko[d]

a ROR Universidad Autónoma del Carmen • KHW-2538-2024 • 0009-0006-2955-0382 • 1231951
b ROR Universidad Autónoma del Carmen • KHW-2160-2024 • 0000-0001-9743-0434 • 49334
c ROR Universidad Autónoma del Carmen • AFN-6960-2022 • 0000-0001-5287-1594 • 292367
d ROR Universidad Autónoma del Carmen • KHW-2340-2024 • 0000-0001-6358-2130 • 798108

CONAHCYT classification:

Area: Engineering
Field: Engineering
Discipline: Mechanical Engineering
Subdiscipline: Materials Mechanics

https://doi.org/10.35429/JEA.2024.32.11.36.42

History of the article:
Received: September 11, 2024
Accepted: December 24, 2024

* ✉ [222524@mail.unacar.mx]

Abstract

The present research focuses on analyzing the uniaxial compressive strength of rocks and its relationship with point load index testing. It is important to note that Seybaplaya, located in Campeche Mexico, is recognized for its fishing, industrial and commercial activities and where a rock bench is located from which samples were obtained to carry out the study. As a result, equations were developed that allow predicting the simple uniaxial compressive strength based on the values obtained from the point load index test. It is relevant to highlight that these relationships are valid only for rocks with lithological characteristics similar to those used in this study. The analysis results and conclusions demonstrate the linearity of the relationships between the simple uniaxial compressive strength and the point load index test.

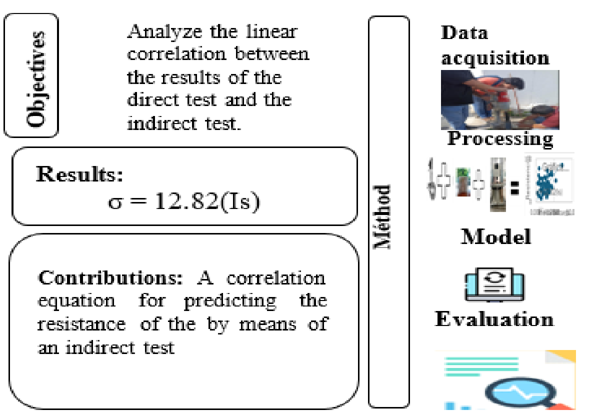

Simple uniaxial compressive strength and rock point load index

Resumen

La presente investigación se enfoca en analizar la resistencia a la compresión uniaxial de las rocas y su relación con ensayo índice de carga puntual. Es importante señalar que Seybaplaya se ubicado en Campeche México, es reconocido por sus actividades pesqueras, industriales, comerciales y en la que se localiza un banco de roca de la que se obtuvieron muestras para llevar a cabo el estudio. Como resultado, se desarrollaron ecuaciones que permiten predecir la resistencia a la compresión uniaxial simple basándose en los valores obtenidos ensayo índice de carga puntual. Es relevante destacar que estas relaciones son válidas únicamente para rocas con características litológicas similares a las utilizadas en este estudio. Los resultados del análisis y las conclusiones demuestran la linealidad de las relaciones entre la resistencia a la compresión uniaxial simple y el ensayo índice de carga punctual

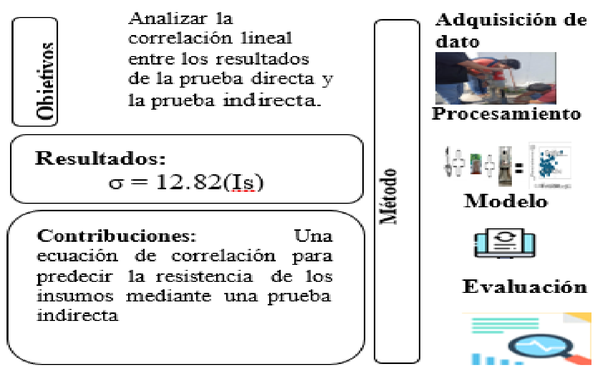

Resistencia a la compresión uniaxial simple e índice de carga puntual de roca

Citation: Naal-Pech, José Wilber, Palemón-Arcos, Leonardo, El-Hamzaoui, Youness and Gutiérrez-Can, Yuriko. Study of the relationship between uniaxial compressive strength and the point load index test in rocks from the bank in Seybaplaya Campeche Mexico. Journal of Engineering Applications. 2024. 11-32: 36-42.

Introduction

Every construction project is based on a soil or rock terrain, with rocks being the fundamental raw material. It is crucial to assess their strength when analysing and designing structures, as this ensures stability from the foundation. In summary, the strength of rocks is a key factor in structural design, as they are natural, hard and compact aggregates, consisting of mineral particles with permanent cohesive bonds. The proportion of different minerals, the granular structure, the texture and the origin of the rock serve for its geological classification (González, 2002).

The behaviour of a block or mass of rock at its place of origin differs from a sample of rock material, which shows significantly higher strength. In addition, blocks of rock often exhibit structural weaknesses, known as cleavages, which include fractures, fissures, joints and other discontinuities. Virtually all of the rocks that make up the kilometres of the earth's crust are traversed by fissures and cracks of short extent (Iriondo, 2006). The diversity in structure, rock types and their geographical distribution affects structural damage in engineering works. Therefore, it is essential to identify these factors in advance, adapt land use according to their impact and reduce the vulnerability of constructions. This problem is the subject of this research focused on the characterisation and mitigation of geological risks caused by geomorphology, specifically in karst areas, such as those found in the state of Campeche (Palacio, 2013).

Due to the high cost and complexity associated with performing the Resistance to Uniaxial Simple Compression (RCUS) test to evaluate the behaviour of rocks, it is recommended to use tests that allow classifying the physical properties of the rocks involved (Naal-Pech et al., 2023). This classification will allow subsequent grouping and characterisation of the rocks by assigning mechanical behaviour parameters that are obtained from tests on representative samples. Determining the simple compressive strength of a rock is important because it allows the rock to be classified according to its strength; it is an important parameter in the most commonly used fracture criteria (Delgado, 2013). Sometimes, it is necessary to ignore the normative recommendations due to discontinuities in the rock mass, which make it difficult to obtain rock cylinders of adequate length.

In addition, for rocks with grains larger than one centimetre, such as granites or pegmatites, obtaining adequate samples may be impossible, and if they are obtained, they cannot be broken with conventional presses. To address these difficulties, researchers such as (Galván, 2011) have developed an experimental correlation between rock compressive strength and indirect test results or physical characteristics of the rock under study, allowing indirect estimates of rock strength to be obtained cheaply and quickly. Equations based on test results relating parameters have been developed using statistical methods of correlation and linear regression. To estimate the simple compressive strength of a rock, there are methods and tests applicable both in the field and in the laboratory, with variations ranging from subjective estimates to indirect measurements. One of the methods used is to obtain the Compressive Strength at Uniaxial Simplex (RCUS) through the index properties of the rock (Galván, & Restrepo, 2016).

These correlations were derived from numerous tests and analyses of rock cores, which allows characterising and relating specific rock parameters. Several researchers have worked hard to obtain these correlation equations in rocks, which were evaluated both in the laboratory and in the field, allowing to relate the uniaxial compressive strength (RCUS) and the point load index. See **Table 1**.

Box 1

Table 1

Correlation equations between compression uniaxial simplex (RCUS) in MPA and point load rating.

Year	Authors	Correlation Equation
1964	D'Andrea et al.	$RCUS=15.3*Is_{(50)}+16.3$
1966	Deere and Miller	$RCUS=20.7*Is_{(50)}+29.6$
1972	Broch and Franklin	$RCUS=24*Is_{(50)}$
1975	Bieniawski	$RCUS=23*Is_{(50)}$
1980	Hassani et al.	$RCUS=29*Is_{(50)}$
1981	Singh	$RCUS=18.7*Is_{(50)}-13.2$
1984	Gunsallus and Kulhawy	$RCUS=16.5*Is_{(50)}+51.0$
1990	Cargill and Shakoor	$RCUS=23*Is_{(50)}+13$
1992	Grasso et al.	$RCUS=25.67*[Is_{(50)}]^{0.57}$
1994	Ulusay et al.	$RCUS=19*Is_{(50)}+12.7$
2001	Kahraman	$R=8,41*Is_{(50)}+9.51$
2003	Quane and Russel	$RCUS=3.86*[Is_{(50)}]^2+5.62*Is_{(50)}$
2004	Tsiambaos and Sabatakakis	$RCUS=7.3*[Is_{(50)}]^{1.71}$
2005	Fener et al	$RCUS=9.08*Is_{(50)}+39.32$
2007	Akram, M. y Bakar, M.Z.A.	RCUS=22.7921*Is(50)+ 13.295
2007	Akram, M. y Bakar, M.Z.A.	RCUS=11.076*Is(50)
2008	Cobanoglu, I. y Celik, S,B.	S,B. RCUS=8.66*Is(50)+1 0.85

ISSN: 2410-3454.
RENIECYT-CONAHCYT: 1702902

Naal-Pech, José Wilber, Palemón-Arcos, Leonardo, El-Hamzaoui, Youness and Gutiérrez-Can, Yuriko. Study of the relationship between uniaxial compressive strength and the point load index test in rocks from the bank in Seybaplaya Campeche Mexico. Journal of Engineering Applications. 2024. 11-32: 36-42
https://doi.org/10.35429/JEA.2024.32.11.36.42

Study area

The main wealth of the state of Campeche comes from important hydrocarbon deposits on its marine shelf, as well as significant deposits of non-metallic minerals such as limestone, gypsum, clays, salt and stone aggregates (Servicio Geológico Mexicano, 2021).

Seybaplaya is located on the 'Yucatan Platform', an extension of sedimentary rock on the Yucatan Peninsula, which was formed by the accumulation of marine sediments millions of years ago and reaches a depth of approximately 200 metres. Its soil is composed mainly of limestone and clay, and the area is home to oil and natural gas deposits, which are critical to the local economy.

It is essential to analyse the rock characteristics of the bench located in and around Seybaplaya, known as Mary Carmen, where a quarry is located. **Figure 1** shows the geographic location of the rock bank, while **Table 2** details the type of material and its volume.

Box 2

Figure 1

Seybaplaya rock bank location in Campeche state, Mexico**.**

Box 3

Tabla 2

Characteristics of the Bank in seybaplaya called Mary Carmen

State:	Campeche		
Name of the bank:	Mar and Carmen		
Kilometre:	1000		
Location:	PAYUCAN		
Coordinates UTM	X 741570.00		Y 2174740.00
Deviation:	Right	Metres:	0
Type of property:			
Type of material:	TEZONTLE		
Treatment:			
Volume x 1000 (m³):	500	Clearance thickness (m):	0.2
Likely uses:			
Use of explosives:	Unrestricted		There are no
Economic aspects:	Convenient	Quality report:	Reporte

Methodology

The most commonly used indirect destructive test on rocks is point load index and the most commonly used direct destructive test is simple uniaxial compressive strength. A systematic framework is presented to analyse the relationship between the uniaxial compressive strength and the indirect destructive test (point load index) on rocks from the Mary Carmen bench at Seybaplaya, Campeche. To achieve this objective and to ensure a structured and logical process, the steps to be followed are detailed below:

- Bench exploration and exploitation
- Sample extraction and preparation
- Indirect test (point load index)
- Simple uniaxial compressive strength test (RCUS).

Each phase is broken down in this section:

Exploration and bench mining

For soil exploration, methods such as open pit, post hole and auger are commonly used. However, in rock bank exploration, drilling methods are used which are often very expensive. Rock benches must be sampled randomly; however, some institutions set the number of drill holes according to the volume of material to be exploited, without considering the homogeneity or heterogeneity of the formation.
Sample extraction and preparation A standard procedure is established for the preparation of rock core samples according to ASTM 2008 D4543.370238-1. Samples should be straight circular cylinders with a length to diameter ratio of 2.0 to 2.5 and a minimum diameter of 47 mm. In addition, the ends must be polished and flat, with a maximum tolerance of 0.001 inch, in this investigation 50 samples of 53.0 mm were used.

Indirect test (point load index)

The Point Load Test (PLT) is performed according to ASTM D5731-05. This test is also known as the Franklin test and was introduced in 1970. It is one of the most widely used indirect tests to determine the strength of rock. This test is performed by applying a point load of compression along its diameter to a cylindrical rock sample until failure. The load is applied by means of two truncated-metallic cones in coaxial and opposite position to each other and the cone dimension is standardised as shown in **Figure 2.**

ISSN: 2410-3454.
RENIECYT-CONAHCYT: 1702902

Naal-Pech, José Wilber, Palemón-Arcos, Leonardo, El-Hamzaoui, Youness and Gutiérrez-Can, Yuriko. Study of the relationship between uniaxial compressive strength and the point load index test in rocks from the bank in Seybaplaya Campeche Mexico. Journal of Engineering Applications. 2024. 11-32: 36-42
https://doi.org/10.35429/JEA.2024.32.11.36.42

Journal of Engineering Applications December 2024 Vol.11 No.32 36-42
Article

Box 4

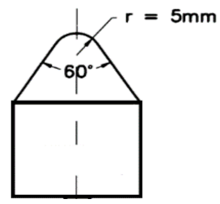

Figure 2
Standardised truncated cone for point load index test.

The uncorrected point load index is calculated with equation 1

$$Is=P*1000/(D_e)^2 \quad (1)$$

Where:
P= Load applied in (kN)
D_e = Distance between load-bearing conical tips (mm)
Is = Point load index, uncorrected (Mpa).

Resistance to simple uniaxial compression test (RCUS). The uniaxial compression test in accordance with ASTM D7012-10. The method used to calculate the uniaxial compressive stress, Poisson's ratio and Young's modulus of a rock core (Peng and Zhang, 2007). The simple uniaxial compressive strength is calculated with equation (2).

$$\sigma=RCUS = P/A \quad (2)$$

Where:
σ = RCUS = simple uniaxial compressive strength in Mpa.
P = axial load N
A = Cross-sectional area ^{mm2}
Simple compression test procedure.

Note the dimensions for evaluating the cross-sectional area.

Ensure that the universal machine is calibrated correctly and in optimum condition, with the reading at zero before starting any measurements. Position the specimen so that it is perfectly centred between the compression platens of the universal machine. Use the control software to program the machine and run the compression test properly. Carry out the test until failure of the specimen is detected, watching carefully for cracks. Remove the load from the specimen. Remove the specimen from the machine and proceed to place a new specimen, repeating the procedure described above (Nieto & Avendaño, 2015).

Results

In this research, 50 single uniaxial compressive strength tests (RCUS) and 50 point load index tests (PLT or Is) were carried out, and the following results were obtained (see **Table 3)**

Box 5

Table 3
Results of the 50 samples: where ID is the identification number of the sample, Rcus in MPA, Is in MPA.

ID	Point loading rate (PLT or Is) in MPA	RCUS single uniaxial compressive strength in MPA
1	3.248	31.6
2	1.283	28.6
3	0.888	46.8
4	0.772	15.2
5	1.912	18.3
6	2.964	11.7
7	1.743	22.7
8	3.143	42.1
9	1.797	53.4
10	0.969	14.9
11	4.339	68.6
12	1.486	8.6
13	1.817	23.2
14	3.548	40.7
15	3.468	43.5
16	3.590	28.7
17	1.949	43.6
18	1.119	55.5
19	1.880	32.3
20	0.854	61.3
21	0.960	78
22	3.459	61.9
23	1.051	42.4
24	5.468	49.1
25	7.117	84.7
26	3.167	72.8
27	2.616	38.1
28	4.477	33.2
29	2.469	58
30	3.109	23.9
31	0.522	21.3
32	1.424	40
33	3.519	34.8
34	2.145	43.6
35	2.833	18.5
36	2.836	54.1
37	3.345	45.5
38	2.985	44.1
39	2.298	22.4
40	3.635	35.1
41	0.551	43.4
42	2.563	37.4
43	3.007	31
44	4.305	36.5
45	4.461	63.7
46	3.086	15.7
47	2.557	57.6
48	3.601	40.5
49	4.032	65.1
50	3.731	23.3

ISSN: 2410-3454.
RENIECYT-CONAHCYT: 1702902

Using information from **Table 3** to correlate RCUS and (PLT or Is), in rock samples from the Seybaplaya bench, we obtain the graph, see **Figure 3**. It is observed that the load and compression index test value, there is an acceptable ^{R2} of 0.7649.

Box 6

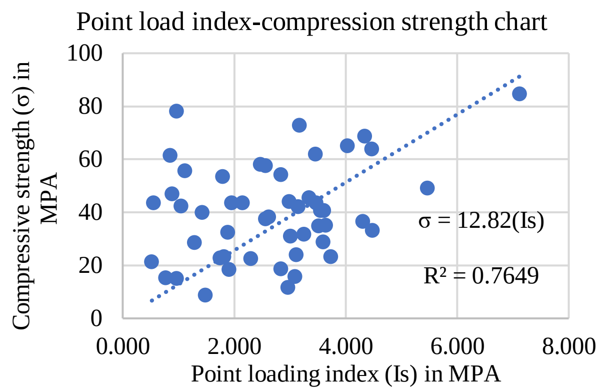

Figura 3

Correlation plot between RCUS and load index value (PLT) in rock samples

Discussion

With the assistance of an expert, explosives were used to mine the bench and rock fragments of considerable diameter were randomly selected for sampling. During the extraction phase, it was observed that the drilling rate varied according to the hardness of the rocks, a fact that was confirmed by compression tests and the identification of the samples by their ID. In addition, it was noted that when water was injected into the borehole, a white liquid was generated, indicating the presence of limestone in the rock. Two samples were extracted from the same fragment: one for the point load test and one to assess the compressive strength.

The compression test specimens were measured with a vernier caliper and cross-sections were made. This process was complicated in some cases due to the disintegration of the specimens, which led to the length ratio of 2 to 2.5 times their diameter not being met, forcing another specimen to be drilled to satisfy the requirements. On the other hand, the samples tested for the point load index were also measured with a vernier caliper, complying with the length - diameter ratio of 1, as established in the standard.

For the load index test on rock samples, diametrically shaped tests were carried out on cylindrical samples.

The uncorrected point load resistance index (Is) was determined. This index was obtained by subjecting a rock sample to a concentrated point load, applied through a pair of truncated conical plates, until fracture occurs in the sample. Compression tests were carried out in the universal machine using dry samples, obtaining the expected results, allowing to observe consistent results throughout the process.

a) It is observed that the rocks present numerous discontinuities.
b) When examining the RCUS-PLT graph, it can be seen that there is an acceptable relationship.
c) When analysing the RCUS-PLT graph, it is observed that the correlation is linear.
d) It is shown that the dynamite bench mining method also creates micro-cracks that continue to damage the resistors.
e) It was observed that the bench material is of limestone type.

Conclusion

The results obtained in this study represent a significant advance in rock mechanics in the state of Campeche. It is fundamental to take into account that the regression models presented in this document are applicable and representative for rocks with similar characteristics to those used in this research. Among the general conclusions, the following considerations stand out: the physico-mechanical parameters of the rock samples analysed in the study were determined. A summary of the ranges of these values is presented below. See **Table 4**.

Box 7

Table 4

Range of RCUS values and PLTen rock samples from the Seybaplaya bench

Concept	Rango	Mean value	Standard deviation	Units
RCUS en MPA	8.6 <> 84.7	40.14	17.9977663	Mpa
Value PLT	0.52<>7.12	2.68	1.35	Mpa

Declarations

Conflict of interest

The authors and co-authors declare that they have no conflicts of interest. They have no competing financial interests or personal relationships that could influence the content of this article.

Naal-Pech, José Wilber, Palemón-Arcos, Leonardo, El-Hamzaoui, Youness and Gutiérrez-Can, Yuriko. Study of the relationship between uniaxial compressive strength and the point load index test in rocks from the bank in Seybaplaya Campeche Mexico. Journal of Engineering Applications. 2024. 11-32: 36-42
https://doi.org/10.35429/JEA.2024.32.11.36.42

Availability of data and materials

The data obtained from this research are available for consultation at any time as needed.

Funding

No internal or external funding was provided for this research project; however, it was possible thanks to the scholarship for postgraduate studies and thanks to the stimulus for belonging to the National System of Researchers and the Programme for the Professional Development of Teachers through the Autonomous University of Carmen (UNACAR).

Authors' contribution

Naal-Pech, José Wilber: Contributed significantly to the conceptualization of the project, as well as to the development of the research method and technique. Supported the design of the field instrument and carried out the data analysis, systematizing the results. In addition, he was in charge of writing the article.

Palemón-Arcos, Leonardo: Carried out the background research for this article and provided support in the design of the field instrument. In addition, he contributed to the writing of the article

El-Hamzaoui, Youness: Contributed to data processing and the generation of correlation graphs, as well as the development of the approach, method and writing of the article

Gutiérrez-Can, Yuriko: Contributed to the research design, defining the type and focus of the study, as well as the development of the method and writing of the article

Acknowledgements

The authors José Naal-Pech, Leonardo Palemón-Arcos and Youness El Hamzaoui are grateful for the support of the Consejo Nacional de Humanidades, Ciencias y Tecnologías (CONAHCYT) provided through the Universidad Autónoma del Carmen (UNACAR). Yuriko Gutiérrez-Can acknowledges the support of the Programa para el Desarrollo Profesional Docente (PRODEP), through the Universidad Autónoma del Carmen and the Grupo Disciplinar de Ingeniería Civil of the UNACAR. All authors are grateful to the Universidad Autónoma de Campeche for the facilities provided to carry out the tests in its structure laboratory.

Abbreviations

ASTM American Society for Testing and Materials.

RCUS Compressive Strength Uniaxially Simple Compressive Strength.

PLT Point Load Test

References

Background

C. Delgado, Evaluación de un cambio Tecnológico para el Procesamiento de Minerales de Alta Dureza. Tesis. Universidad de Chile: 2013.

Galván, M., Correlación entre la resistencia a compresión simple y el índice a carga puntual Is (50) en calizas de la Comunidad Valenciana (España). Tesis Doctoral, Universidad Politécnica de Valencia, España, 2011.

González de Vallejo L. I., Ferrer M., Ortuño L., Oteo C., (2002) Ingeniería Geológica, Editorial Pearson Educación, Madrid, ISBN84-205-3104-9.

M. Galván, I. Restrepo, «Correlación de la resistencia a compresión uniaxial con la humedad y porosidad eficaz en rocas». DYNA. 2016.

M. Iriondo, Introducción a la Geología. Córdova. Argentina: 2006.Editorail Brujas, argentina ISBN-978-987-591-061-4

Naal-Pech, José W., Palemón-Arcos, Leonardo, El Hamzaoui, Youness and Gutiérrez-Can, Yuriko. 2023. Study of the relationship between uniaxial compressive strength, water content, porosity and density in bank rocks in Seybaplaya Campeche. Doi: 10.35429/JME.2023.20.7.9.16. Vol.7 No.20 9-16.

Palacio Aponte A. G., 2013. Identificación y Caracterización de la Subsidencia y/o Colapso de Terrenos Kásrticos. P. 169-181. En: Posada Vanegas G., B.E. Vega Serratos, y Silva Casarín (eds), Peligros Naturales en el Estado de Campeche. Cuantificación y Protección Civil. Universidad Autónoma de Campeche, cenecam-Gobierno del Estado de Campeche, cenapred.

Servicio Geológico Mexicano (sgm)., 2021 Panorama Minero del Estado de Campeche.

ISSN: 2410-3454.
RENIECYT-CONAHCYT: 1702902

Basics

ASTM 05 Standards, Standard: D 5731-05. Test Method for Determination of the Point Load Strength Index of Rock.

ASTM 2008. Standard Practices for Preparing Rock Core as Cylindrical Test Specimens and Verifying Conformance to Dimensional and Shape Tolerances. D4543.370238-1.

ASTM 2010a. Standard Test Method for Compressive Strength and Elastic Moduli of Intact Rock Core Specimens under Varying States of Stress and Temperatures. D7012-10

Nieto, G. C., & Avendaño, D. P. (2015). Guía de laboratorio de Resistencia de materiales. Bogota D.C: Inimagdalena

Peng, S. and Zhang, J., Rock properties and mechanical behaviors. Engineering Geology for Underground Rocks. Springer Berlin Heidelberg, 2007.

Supports

Çobanoğlu and S. B. Çelik (2008): Estimation of uniaxial compressive strength from point load strength, schmidt hardness and P-wave velocity, Bulletin of Engineering Geology and the Environment, 67: 491–498.

Bieniawski ZT (1975) Point load test in geotechnical practice. Eng Geol 9(1):1–11

Broch E, Franklin JA (1972) Point-load strength test. Int J Rock Mech Min Sci 9(6):669–697

D'Andrea DV, Fisher RL, Fogelson DE (1964) Prediction of compression strength from other rock properties. Col Sch Mines Q 59(4B):623–640

Deere DU, Miller RP (1966) Engineering classification and index properties for intact rock. Air Force Weapons Lab. Technical report, AFWL-TR 65–116, Kirtland Base, New Mexico

Fener M, Kahraman S, Bilgil A, Gunaydin O (2005) A comparative evaluation of indirect methods to estimate the compressive strength of rocks. Rock Mech Rock Eng 38(4):329–343

Grasso P, Xu S, Mahtab A (1992) Problems and promises of index testing of rocks. In: Tillerson JR, Wawersik WR (eds) Proceed ings of the 33rd US symposium on rock mechanics. Balkema, Rotterdam, pp 879–888

Gunsallus KL, Kulhawy FH (1984) A comparative evaluation of rock strength measures. Int J Rock Mech Min Sci 21:233–248

Hassani FP, Scoble MJ, Whittaker BN (1980) Application of point load index test to strength determination of rock and proposals for new size-correction chart. In: Summers DA (ed) Proceedings of the 21st US symposium on rock mechanics. University of Missouri Press, Rolla, pp 543–564

Kahraman S (2001) Evaluation of simple methods for assessing the uniaxial compressive strength of rock. Int J Rock Mech Min Sci 38:981–994

M. Akram and M. Z. A. Bakar (2007) Correlation between Uniaxial Compressive Strength and Point Load Index for Salt-Range Rocks Pak. J. Engg. & Appl. Sci. Vol. 1 July 2007

Quane SL, Russel JK (2003) Rock strength as a metric of welding intensity in pyroclastic deposits. Eur J Mineral 15:855–864

Singh DP (1981) Determination of some engineering properties of weak rocks. In: Akai K (ed) Proceedings of the international symposium on weak rock. Balkema, Rotterdam, pp 21–24

Tsiambaos G, Sabatakakis N (2004) Considerations on strength of intact sedimentary rocks. Eng Geol 72:261–273.

ISSN: 2410-3454.
RENIECYT-CONAHCYT: 1702902

Naal-Pech, José Wilber, Palemón-Arcos, Leonardo, El-Hamzaoui, Youness and Gutiérrez-Can, Yuriko. Study of the relationship between uniaxial compressive strength and the point load index test in rocks from the bank in Seybaplaya Campeche Mexico. Journal of Engineering Applications. 2024. 11-32: 36-42
https://doi.org/10.35429/JEA.2024.32.11.36.42

[Title in TNRoman and Bold No. 14 in English and Spanish]

Surname, Name 1st Author*[a], Surname, Name 1st Co-author[b], Surname, Name 2nd Co-author[c] and Surname, Name 3rd Co-author[d] [No.12 TNRoman]

[a] Affiliation institution, Researcher ID, ORC ID, SNI-CONAHCYT ID or CVU PNPC [No.10 TNRoman]
[b] Affiliation institution, Researcher ID, ORC ID, SNI-CONAHCYT ID or CVU PNPC [No.10 TNRoman]
[c] Affiliation institution, Researcher ID, ORC ID, SNI-CONAHCYT ID or CVU PNPC [No.10 TNRoman]
[d] Affiliation institution, Researcher ID, ORC ID, SNI-CONAHCYT ID or CVU PNPC [No.10 TNRoman]

CONAHCYT classification:
https://marvid.org/area-i.php [No.10 TNRoman]
Area:
Field:
Discipline:
Subdiscipline:

DOI: https://doi.org/
Article History:
Received: [Use Only ECORFAN]
Accepted: [Use Only ECORFAN]

* ✉ [example@example.org]

Graphical abstract [In English]

Authors must provide an original image that clearly represents the article described in the article. Graphical abstracts should be submitted as a separate file. Please note that, as well as each article must be unique.

Image size: provide an image with a minimum of 1200 x 500 pixels [width x height] using a minimum resolution of 200 dpi.

Font: TNRoman with a sufficiently large font size, as the image will be reduced in size to fit the table of contents in a 250-pixel high window.

File type: the file types are MS Office files.

No additional text, outline or synopsis should be included. Any text or captions must be part of the image file. Do not use unnecessary white space or a "graphic abstract" header within the image file.

Keywords [In English]
Indicate 3 keywords in TNRoman and Bold No. 10

Graphical abstract [In Spanish]

Authors must provide an original image that clearly represents the article described in the article. Graphical abstracts should be submitted as a separate file. Please note that, as well as each article must be unique.

Image size: provide an image with a minimum of 1200 x 500 pixels [width x height] using a minimum resolution of 200 dpi.

Font: TNRoman with a sufficiently large font size, as the image will be reduced in size to fit the table of contents in a 250-pixel high window.

File type: the file types are MS Office files.

No additional text, outline or synopsis should be included. Any text or captions must be part of the image file. Do not use unnecessary white space or a "graphic abstract" header within the image file.

Keywords [In Spanish]
Indicate 3 keywords in TNRoman and Bold No. 10

Citation: Surname, Name 1st Author, Surname, Name 1st Co-author, Surname, Name 2nd Co-author and Surname, Name 3rd Co-author. Article Title. Journal of Engineering Applications. Year. V-N: Pages [TN Roman No.10].

ECORFAN Mexico

RENIECYT
Registro Nacional de Instituciones y Empresas Científicas y Tecnológicas
1702902 CONAHCYT

Introduction

Text in TNRoman No.12, single space.

General explanation of the subject and explain why it is important.

What is your added value with respect to other techniques?

Clearly focus each of its features.

Clearly explain the problem to be solved and the central hypothesis.

Explanation of sections Article.

Development of headings and subheadings of the article with subsequent numbers

[Title No.12 in TNRoman, single spaced and bold]

Products in development No.12 TNRoman, single spaced.

Including figures and tables-Editable

In the article content any table and figure should be editable formats that can change size, type and number of letter, for the purposes of edition, these must be high quality, not pixelated and should be noticeable even reducing image scale.

[Indicating the title at the bottom with No.10 and Times New Roman Bold]

Box

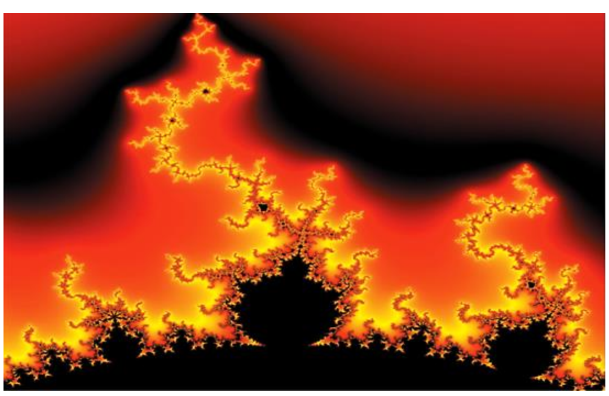

Figure 1
Title [Should not be images-everything must be editable]

Source [in italic]

Box

Table 1
Title [Should not be images-everything must be editable]

Source [in italic]

Each article shall present separately in **2 folders**: a) Figures and b) Tables in .JPG format, indicating the number and sequential Bold Title.

For the use of equations, noted as follows:

$$Y_{ij} = \alpha + \sum_{h=1}^{r} \beta_h X_{hij} + u_j + e_{ij} \quad [1]$$

Must be editable and number aligned on the right side.

Methodology

Develop give the meaning of the variables in linear writing and important is the comparison of the used criteria.

Results

The results shall be by section of the article.

Conclusions

Clearly explain the results and possibilities of improvement.

Annexes

Tables and adequate sources.

Declarations

Conflict of interest

The authors declare no interest conflict. They have no known competing financial interests or personal relationships that could have appeared to influence the article reported in this article.

Author contribution

Specify the contribution of each researcher in each of the points developed in this research.

Availability of data and materials

Indicate the availability of the data obtained in this research.

Funding

Indicate if the research received some financing.

Acknowledgements

Indicate if they were financed by any institution, University or company.

Abbreviations

List abbreviations in alphabetical order.

References

Use APA system. Should not be numbered, nor with bullets, however if necessary numbering will be because reference or mention is made somewhere in the Article.

Use the Roman alphabet, all references you have used should be in Roman alphabet, even if you have cited an article, book in any of the official languages of the United Nations [English, French, German, Chinese, Russian, Portuguese, Italian, Spanish, Arabic], you should write the reference in Roman alphabet and not in any of the official languages.

Citations are classified the following categories:

Antecedents. The citation is due to previously published research and orients the citing document within a particular scholarly area.

Basics. The citation is intended to report data sets, methods, concepts and ideas on which the authors of the citing document base their work.

Supports. The citing article reports similar results. It may also refer to similarities in methodology or, in some cases, to the reproduction of results.

Differences. The citing document reports by means of a citation that it has obtained different results to those obtained in the cited document. This may also refer to differences in methodology or differences in sample sizes that affect the results.

Discussions. The citing article cites another study because it is providing a more detailed discussion of the subject matter.

The URL of the resource is activated in the DOI or in the title of the resource.

Example

Mandelbrot, B. B. [2020]. Negative dimensions and Hölders, multifractals and their Hölder spectra, and the role of lateral preasymptotics in science. Journal of Fourier Analysis and Applications Special. 409-432.

Intellectual Property Requirements for editing:

- Authentic Signature in Color of Originality Format Author and Coauthors.

- Authentic Signature in Color of the Acceptance Format of Author and Coauthors.

- Authentic Signature in blue color of the Conflict of Interest Format of Author and Co-authors.

ISSN: 2410-3454

RENIECYT-CONAHCYT: 1702902

Reservation to Editorial Policy

Journal of Engineering Applications reserves the right to make editorial changes required to adapt the Articles to the Editorial Policy of the Journal. Once the Article is accepted in its final version, the Journal will send the author the proofs for review. ECORFAN® will only accept the correction of errata and errors or omissions arising from the editing process of the Journal, reserving in full the copyrights and content dissemination. No deletions, substitutions or additions that alter the formation of the Article will be accepted.

Code of Ethics - Good Practices and Declaration of Solution to Editorial Conflicts

Declaration of Originality and unpublished character of the Article, of Authors, on the obtaining of data and interpretation of results, Acknowledgments, Conflict of interests, Assignment of rights and Distribution

The ECORFAN-Mexico, S.C. Management claims to Authors of Articles that its content must be original, unpublished and of Scientific, Technological and Innovation content to be submitted for evaluation.

The Authors signing the Article must be the same that have contributed to its conception, realization and development, as well as obtaining the data, interpreting the results, drafting and reviewing it. The Corresponding Author of the proposed Article will request the form that follows.

Article title:

- The sending of an Article to Journal of Engineering Applications emanates the commitment of the author not to submit it simultaneously to the consideration of other series publications for it must complement the Format of Originality for its Article, unless it is rejected by the Arbitration Committee, it may be withdrawn.

- None of the data presented in this article has been plagiarized or invented. The original data are clearly distinguished from those already published. And it is known of the test in PLAGSCAN if a level of plagiarism is detected Positive will not proceed to arbitrate.

- References are cited on which the information contained in the Article is based, as well as theories and data from other previously published Articles.

- The authors sign the Format of Authorization for their Article to be disseminated by means that ECORFAN-Mexico, S.C. In its Holding Bolivia considers pertinent for disclosure and diffusion of its Article its Rights of Work.

- Consent has been obtained from those who have contributed unpublished data obtained through verbal or written communication, and such communication and Authorship are adequately identified.

- The Author and Co-Authors who sign this work have participated in its planning, design and execution, as well as in the interpretation of the results. They also critically reviewed the paper, approved its final version and agreed with its publication.

- No signature responsible for the work has been omitted and the criteria of Scientific Authorization are satisfied.

- The results of this Article have been interpreted objectively. Any results contrary to the point of view of those who sign are exposed and discussed in the Article.

Copyright and Access

The publication of this Article supposes the transfer of the copyright to ECORFAN-Mexico, SC in its Holding Bolivia for it Journal of Engineering Applications, which reserves the right to distribute on the Web the published version of the Article and the making available of the Article in This format supposes for its Authors the fulfilment of what is established in the Law of Science and Technology of the United Mexican States, regarding the obligation to allow access to the results of Scientific Research.

Article Title:

Name and Surnames of the Contact Author and the Co-authors	Signature
1.	
2.	
3.	
4.	

Principles of Ethics and Declaration of Solution to Editorial Conflicts

Editor Responsibilities

The Publisher undertakes to guarantee the confidentiality of the evaluation process, it may not disclose to the Arbitrators the identity of the Authors, nor may it reveal the identity of theArbitrators at any time.

The Editor assumes the responsibility to properly inform the Author of the stage of the editorial process in which the text is sent, as well as the resolutions of Double-Blind Review.

The Editor should evaluate manuscripts and their intellectual content without distinction of race, gender, sexual orientation, religious beliefs, ethnicity, nationality, or the political philosophy of the Authors.

The Editor and his editing team of ECORFAN® Holdings will not disclose any information about Articles submitted to anyone other than the corresponding Author.

The Editor should make fair and impartial decisions and ensure a fair Double-Blind Review.

Responsibilities of the Editorial Board

The description of the peer review processes is made known by the Editorial Board in order that the Authors know what the evaluation criteria are and will always be willing to justify any controversy in the evaluation process. In case of Plagiarism Detection to the Article the

Committee notifies the Authors for Violation to the Right of Scientific, Technological and Innovation Authorization.

Responsibilities of the Arbitration Committee

The Arbitrators undertake to notify about any unethical conduct by the Authors and to indicate all the information that may be reason to reject the publication of the Articles. In addition, they must undertake to keep confidential information related to the Articles they evaluate.

Any manuscript received for your arbitration must be treated as confidential, should not be displayed or discussed with other experts, except with the permission of the Editor.

The Arbitrators must be conducted objectively, any personal criticism of the Author is inappropriate.

The Arbitrators must express their points of view with clarity and with valid arguments that contribute to the Scientific, Technological and Innovation of the Author.

The Arbitrators should not evaluate manuscripts in which they have conflicts of interest and have been notified to the Editor before submitting the Article for Double-Blind Review.

Responsibilities of the Authors

Authors must guarantee that their articles are the product of their original work and that the data has been obtained ethically.

Authors must ensure that they have not been previously published or that they are not considered in another serial publication.

Authors must strictly follow the rules for the publication of Defined Articles by the Editorial Board.

The authors have requested that the text in all its forms be an unethical editorial behavior and is unacceptable, consequently, any manuscript that incurs in plagiarism is eliminated and not considered for publication.

Authors should cite publications that have been influential in the nature of the Article submitted to arbitration.

Information services

Indexation - Bases and Repositories

LATINDEX (Scientific Journals of Latin America, Spain and Portugal)
RESEARCH GATE (Germany)
GOOGLE SCHOLAR (Citation indices-Google)
REDIB (Ibero-American Network of Innovation and Scientific Knowledge- CSIC)
MENDELEY (Bibliographic References Manager)
DULCINEA (Spanish scientific journals)
UNIVERSIA (University Library-Madrid)
SHERPA (University of Nottingham-England)

Publishing Services

Citation and Index Identification H
Management of Originality Format and Authorization
Testing Article with PLAGSCAN
Article Evaluation
Certificate of Double-Blind Review
Article Edition
Web layout
Indexing and Repository
ArticleTranslation
Article Publication
Certificate of Article
Service Billing

Editorial Policy and Management

21 Santa Lucía, CP-5220. Libertadores -Sucre – Bolivia. Phones: +52 1 55 6159 2296, +52 1 55 1260 0355, +52 1 55 6034 9181; Email: contact@ecorfan.org www.
ecorfan.org

Site Licences

03-2010-032610094200-01-For printed material ,03-2010-031613323600-01-For Electronic material,03-2010-032610105200-01-For Photographic material,03-2010-032610115700-14-For the facts Compilation,04-2010-031613323600-01-For its Web page,19502-For the Iberoamerican and Caribbean Indexation,20-281 HB9-For its indexation in Latin-American in Social Sciences and Humanities,671-For its indexing in Electronic Scientific Journals Spanish and Latin America,7045008-For its divulgation and edition in the Ministry of Education and CultureSpain,25409-For its repository in the Biblioteca Universitaria-Madrid,16258-For its indexing in the Dialnet,20589-For its indexing in the edited Journals in the countries of Iberian-America and the Caribbean, 15048-For the international registration of Congress and Colloquiums. financingprograms@ecorfan.org

Management Offices

21 Santa Lucía, CP-5220. Libertadores – Sucre – Bolivia.

Journal of Engineering Applications

"Analysis of solution methods for high order ordinary differential equations used in electrical circuits"

Gutiérrez-Robles, José Alberto, Galván-Sánchez, Verónica Adriana, Bañuelos-Cabral, Eduardo Salvador and De La Cruz-García, Elba Lilia

University of Guadalajara

"Inverter technology and the role of the user behavior: Towards a more efficient use of energy"

Vidal-Santo, Adrián, Campos-Domínguez, Armando, Vázquez-Guzmán, Aldo G. and Castillo-Toscano, William A.

Universidad Veracruzana

"Methodological proposal for the topographic use of UAV compared to the use of traditional methods"

Rodríguez-González, José Miguel, Gómez-Arizmendi, Gabriela, Velázquez-García, Jennyfer and Carranza-Reyes, Roberto

Tecnológico Nacional de México/TES Valle de Bravo

"Study of the relationship between uniaxial compressive strength and the point load index test in rocks from the bank in Seybaplaya Campeche Mexico"

Naal-Pech, José Wilber, Palemón-Arcos, Leonardo, El-Hamzaoui, Youness and Gutiérrez-Can, Yuriko

Universidad Autónoma del Carmen

ISSN 2410 - 3454

www.ecorfan.org